

MOHAMED KHIDER UNIVERSITY OF BISKRA FACULTY OF EXACT SCIENCES Matter Sciences department

MASTER THESIS

Matter Sciences Chemistry Pharmaceutical chemistry

Presented by:

MELLAS NARIMANE

THE:

Theoretical study of the regioselectivity of the transetherification reaction and *in silico* prediction of pharmacological properties of 2-nitroanilines

Jury:

Mr	DAOUD Ismail	Prof	University of Biskra	President
Mr	MELKEMI Nadjib	Prof	University of Biskra	Supervisor
Ms	LEHRAKI Faiza	MA/A	University of Biskra	Examiner

Academic Year: 2024-2025

This dissertation is dedicated to my beloved parents

to my cherished sisters

to my dear uncles and aunts

and to all those who hold a special place in my heart

Acknowledgements

The completion of this work would never have been possible without the support, advice and guidance of many people, to whom I would like to express my sincere gratitude.

First and foremost, I would like to sincerely thank my supervisor, Prof. Melkemi, for his availability, his scientific rigor and his invaluable advice throughout this work. His trust, patience and benevolent guidance have been of great value to me, both professionally and personally. I would like to express my deepest gratitude to him for guiding me with pedagogy and high standards, while respecting my autonomy.

I would like to thank my committee members Mr. Daoud Ismail and Ms. Lehraki Faiza for agreeing to judge this work.

I would also like to express my sincerest thanks to my parents, my dear father and mother, for their unconditional love, patience, constant encouragement and silent prayers. Their moral and emotional support has been the cornerstone of my perseverance over the years. It is largely thanks to them that this work has come to fruition.

I can't forget my dear sisters, Sabrine, Nesrine and Safaa, who have always supported me, listened to me and encouraged me. Their affection and presence have been a great comfort to me.

My grateful thoughts also go to my grandfathers, my aunts and my uncles, for their prayers, their kind words and their discreet but oh-so-important support.

I'd like to extend my heartfelt thanks to my colleague Zineb, for her invaluable collaboration, her attentiveness, her constant support and her infectious good humor. Working alongside her has been a real pleasure and a great advantage in difficult times.

I would also like to thank all the teachers, lecturers and administrative staff who have accompanied me throughout my university career, for the quality of their teaching and their commitment.

Finally, I would like to extend my sincerest thanks to all those who have contributed in any way to the success of this work.

"The best way to have a good idea is to have lots of ideas."

LinusPauling

Abstract

Type 2 diabetes affects over 350 million people worldwide. Even with the availability of medications, regulating blood sugar levels remains difficult. In order to enhance metabolic balance and lower the incidence of problems, novel and efficient treatments are being investigated. SIRT6 is considered an attractive biological target for the development of new type 2 diabetes drugs. Our research work focuses on two main themes.

First, the regioselectivity of the transetherification reaction of 4,5-dialkoxy-2-nitroanilines was theoretically studied using reactivity concepts from the DFT approach. The findings indicate that the carbon atom C4 is the best site for aromatic nucleophilic substitution (ArSN).

The second study aims to identify the binding mechanism of SIRT6 as a potential target for the therapy of type 2 diabetes. Molecular docking was used to explore the interaction of 5-(4-methylpiperazin-1-yl)-2-nitroaniline and its five analogs with the SIRT6 pocket. Molecular docking/Dynamics simulations revealed high binding affinity for ligands L4 and L18, as well as stable interactions with the pocket of the SIRT6 (PDB ID: 3K35). This affinity was confirmed by high negative score values and the establishment of several non-covalent interactions with the active site residues of the receptor. Furthermore, drug-likeness and ADME prediction analyses showed favourable absorption and oral bioavailability characteristics for ligands L4 and L18, suggesting their potential as precursor compounds for antidiabetic drug development.

These analyses have led to a better understanding of the experimentally observed chemical behaviour and open up promising prospects in the field of pharmaceutical compound design.

Keywords: 2-nitroaniline, Regioselectivity, Transetherification reaction, DFT, SIRT6, Molecular docking/Dynamics simulations, ADME.

Résumé

Le diabète de type 2 touche plus de 350 millions de personnes dans le monde. Malgré la disponibilité des médicaments, la régulation de la glycémie reste difficile. Afin d'améliorer l'équilibre métabolique et de réduire l'incidence des problèmes, de nouveaux traitements efficaces sont à l'étude. SIRT6 est considérée comme une cible biologique intéressante pour le développement de nouveaux médicaments contre le diabète de type 2. Nos travaux de recherche s'articulent autour de deux axes principaux.

Tout d'abord, la régiosélectivité de la réaction de transéthérification des 4,5-dialcoxy-2-nitroanilines a été étudiée théoriquement à l'aide des concepts de réactivité issus de l'approche DFT. Les résultats indiquent que l'atome de carbone C4 est le site le plus favorisé pour la substitution nucléophile aromatique (ArSN).

La deuxième étude vise à identifier le mécanisme de liaison de SIRT6 comme cible potentielle pour le traitement du diabète de type 2. Le docking moléculaire a été utilisé pour explorer les interactions de 5-(4-méthylpipérazin-1-yl)-2-nitroaniline et de ses cinq analogs avec le site actif de SIRT6. Les simulations de docking/dynamique moléculaire ont révélé une forte affinité de liaison pour les ligands L4 et L18, ainsi que forment des interactions stables avec la poche du récepteur SIRT6 (PDB ID : 3K35). Cette affinité a été confirmée par des scores négatifs élevés et l'établissement de plusieurs interactions non covalentes avec les résidus du site actif du récepteur. De plus, les analyses de Druglikeness et de prédiction ADME ont montré des caractéristiques d'absorption et de biodisponibilité orale favorables pour les ligands L4 et L18, suggérant leur potentiel d'être des composés précurseurs pour le développement des médicaments antidiabétiques.

Ces analyses ont permis de mieux comprendre le comportement chimique observé expérimentalement et ouvrent des perspectives prometteuses dans le domaine de la conception de composés pharmaceutiques.

Mots clés : 2-nitroaniline, Regioséléctivité, Reaction de transetherification, DFT, SIRT6, simulations docking/dynamique moléculaire, ADME.

Contents

LIST OF MAIN ABBREVIATIONS	IX
LIST OF FIGURES	X
LIST OF TABLES	XII
GENERAL INTRODUCTION	1
References	3
LIST OF FIGURES	
NITROANILINE COMPOUNDS	
PART 1: OVERVIEW OF DIABETES	5
I.1.1. Introduction	5
I.1.2 DIABETES DEFINITION	6
I.1.3. CLASSIFICATION AND PATHOPHYSIOLOGY	6
I.1.4. DIAGNOSIS AND TREATMENT	7
I.1.5. PHARMACEUTICAL RESEARCH AND INNOVATION	8
PART 2: OVERVIEW OF NITROANILINE COMPOUNDS	9
I.2.1. DEFINITION	9
I.2.2. NITROANILINE - STRUCTURE AND MOLECULAR PROPERTIES	9
I.2.3. Physico-chemical properties	10
I.2.4. CHEMICAL REACTIVITY	10
I.2.5. TOXICITY AND SAFETY	10
I.2.6. INDUSTRIAL AND SCIENTIFIC APPLICATIONS	10
I.2.7. Aromatic substitution reactions	11
I.2.8. CLASSICAL NUCLEOPHILIC AROMATIC SUBSTITUTION	11
I.2.9. MECHANISM OF NUCLEOPHILIC AROMATIC SUBSTITUTION	12
References	14

CHAPTER II: THEORETICAL STUDY ON THE REGIOSELECTIVITY OF THE TRANSETHERIFICATION OF 4,5-DIALKOXY-2-NITROANILINE

II.1. Introduction	17
II.2. COMPUTATIONAL METHODS:	18
II.3. Frontier molecular orbitals (HOMO and LUMO)	18
II.4. GLOBAL AND LOCAL REACTIVITY DESCRIPTORS	20
II.4.1. Global HSAB (Hard and Soft Acids and Bases) principle	20
II.4.1.1. Definitions	20
II.4.1.2. Statement of the HSAB principle	21
II.4.2 Chemical concepts and reactivity indices derived from DFT	22
II.4.2.1 Global Indices derived from conceptual DFT	22
a) Electronic Chemical Potential	23
b) Global Hardness and Softness	23
c) Global Electrophilicity Index	23
d) Global Nucleophilicity Index	23
II.4.2.2 Local reactivity indices derived from conceptual DFT	25
a)Fukui Indices	26
b)Condensed Form of Fukui Functions	26
II.5. MOLECULAR ELECTROSTATIC POTENTIAL (MEP)	29
a)3D-Molecular Electrostatic Potential	29
b)2D-Contours of the Molecular Electrostatic Potential	29
II.6. CONCLUSION	31
Reference	32
CHAPTER III:IN SILICO STUDY OF THE ANTID	IABETIC
PROPERTIES OF 5-(4-METHYLPIPERAZIN-1-	·YL)-2-
NITROANILINE AND ITS ANALOGS.	
III.1. Introduction	35
III.2. Brief overview of <i>in silico</i> methods in drug discovery	35
III.2.1. Molecular docking	35
III.2.2. Types of molecular docking	36
III.2.3. Molecular docking procedure	37

a. Ligand preparation	37
b. Target preparation	37
c. Active site recognition	37
d. Docking	38
e. Validation and evaluation	38
III.2.4. Molecular Dynamics (MD) simulations	38
III.2.5. Bioisosteric Conversion	39
III.3. MOLECULAR DOCKING/DYNAMICS SIMULATIONS OF 5-(4-METHYLPIPERA	AZIN-1-YL)-2-
NITROANILINE AND ITS ANALOGS AS SIRT6 INHIBITORS	39
III.3.1. Materials and methods	39
III.3.1.1 Ligands preparation	39
III.3.1.2. Target preparation	40
III.3.1.3. Molecular docking protocol	42
Active site residues of target	42
Method validation	43
III.3.1.3. Molecular Dynamicss simulation	43
III.3.1.4. ADME prediction and physicochemical properties	44
III.3.2. Results and discussion	44
III.3.2.1. Molecular docking analysis	44
III.3.2.2. Molecular Dynamicss analysis	50
III.3.2.3. Protein-ligand interactions after MD simulations	52
III.3.2.4. Evaluation of the ADME-T properties and drug-likeness:	
References.	
GENERAL CONCLUSION	
GENERAL CONCLUSION	39

List of main abbreviations

ADME: Absorption, Distribution, Metabolism, Elimination

BBB: Blood-Brain Barrier

CYP: Cytochrome Enzyme

DFT: Density Functional Theory

FF: Fukui Function

FMO: Frontier Molecular Orbitals Approximation

GI: Gastrointestinal Absorption

HOMO: Highest Occupied Molecular Orbital

HPA: Hirschfeld Population Analysis

HSAB: Hard and Soft Acids and Bases

ICD: Intracellular Domain

LUMO: Lowest Unoccupied Molecular Orbital

MD: Molecular Dynamics

MEP: Molecular Electrostatic Potential

MOE: Molecular Operating Environment

PDB: Protein Data Bank

P-gp: Permeability Glycoprotein

RMSD: Root-Mean-Square Deviation

SF: Scoring Function

SAR: Structure Activity Relationship

List of figures

Chapter I

FIGURE I. 1: TYPES OF DIABETES VECTOR ILLUSTRATION DIAGRAM SCHEME	7
FIGURE I. 2: HIGH BLOOD GLUCOSE NORMAL GLUCOSE DESIGN VECTOR ILLUSTRATION	8
FIGURE I. 3 : STRUCTURE OF 2-NITROANILINE.	9
FIGURE I. 4 : CLASSICAL TWO-STEP MECHANISM FOR SNAR REACTIONS	11
FIGURE I. 5 : SOME KNOWN MEISENHEIMER INTERMEDIATES	12
Chapter II	
FIGURE II. 1: TRANSETHERIFICATION REACTIONS OF 2-NITROANILINES	17
FIGURE II. 2: FRONTIER MOLECULAR ORBITALS PLOTS OF 4,5-DIALKOXY-2-NITROANILINES .	20
FIGURE II. 3: DUAL DESCRIPTOR 3D-MAPPED SURFACES, MAPPED THROUGH (FMO)	
APPROXIMATION.	28
FIGURE II. 4: 3D-MESP SURFACE MAP AND 2D-MESP CONTOUR MAP FOR 4,5-DIALKOXY-2-	-
NITROANILINES	31
Chapter III	
FIGURE III. 1: DIFFERENT TYPES OF MOLECULAR DOCKING STUDIES BASED ON FLEXIBILITY O	F
RECEPTORS/LIGANDS CONSIDERED IN MOLECULAR INTERACTION	36
FIGURE III. 2: STRUCTURE OF 5-(4-METHYLPIPERAZIN-1-YL)-2-NITROANILINE	39
FIGURE III. 3: STRUCTURES OF THE 5-(4-METHYLPIPERAZIN-1-YL)-2-NITROANILINE ANALOG	S
	40
FIGURE III. 4: 3D STRUCTURE OF THE 3K35 ENZYME.	41
FIGURE III. 5: ACTIVE SITE OF THE SELECTED TARGET.	42
Figure III. 6: $3D$ crystal structure of $3K35$ complexed with APR (co-crystallized	
LIGAND) AND $2D$ REPRESENTATION OF THE INTERACTIONS OF APR WITH THE BINDING	
POCKET OF 3K35.	43
FIGURE III. 7: 2D AND 3D INTERACTIONS FORMED BETWEEN THE SYNTHESIZED COMPOUND	
AND THE BEST ANALOGS (L1, L4, L13, L17 and L18) WITH THE ACTIVE SITE RESIDUES O	F
THE SIRT6 RECEPTOR (3K35).	50
FIGURE III. 8: POTENTIAL ENERGY PLOT OF THE SYNTHESIZED COMPOUND AND THE TOP-	
SCORING FIVE HITS WITH 3K35 AS A FUNCTION OF SIMULATION TIME	51

FIGURE III. 9: 2D INTERACTIONS FORMED AFTER MOLECULAR DYNAMICSS SIMULATION	
BETWEEN THE SYNTHESIZED COMPOUND AND THE BEST ANALOGS (L1, L4, L13, L17 and	
L18) WITH THE ACTIVE SITE RESIDUES OF THE SIRT6 RECEPTOR (3K35)	3

List of Tables

Chapter II

TABLE II. 1 : CHEMICAL STRUCTURE 4,5-DIALKOXY-2-NITROANILINES UNDER STUDY
TABLE II. 2: HARD/SOFT CHARACTERISTICS IN HSAB PRINCIPALE 2
TABLE II. 3 : VALUES OF HOMO-LUMO GAP (Δ), GLOBAL REACTIVITY INDICES (X, H, S, Ω , N)
AND DIPOLE MOMENT (DM).
TABLE II. 4: HIRSHFELD ATOMIC CHARGE AND CONDENSED FUKUI FUNCTIONS $f^+(r)$ OF THE C4 AND C5 ATOMS OF 4,5-DIALKOXY-2-NITROANILINES UNDER STUDY
Chapter III
TABLE III. 1- SOME CHARACTERISTICS OF THE TARGETS SELECTED FOR THE STUDY. 4.2
TABLE III. 2: INFORMATION OF THE SELECTED TARGET (3K35)
TABLE III. 3: DOCKING SCORE ENERGY, RMSD, AND INTERACTIONS BETWEEN COMPOUNDS
AND APR WITH RESIDUES OF THE ACTIVE SITE RESIDUES OF THE 3K35 TARGET45
TABLE III. 4: RESULTS OF A MOLECULAR DYNAMICSS STUDY OF THE BEST SCORE OF THE SIX
LIGANDS IN THE ACTIVE SITE OF 3K35
TABLE III. 5: ADME AND DRUG LIKENESS PROPERTIES FOR THE SYNTHESIZED COMPOUND AND
FIVE BEST ANALOGS55

GENERAL INTRODUCTION

Recent advances in pharmaceutical chemistry increasingly rely on the synergy between classical experimental approaches and theoretical methods derived from computational chemistry. This integration provides an in-depth understanding of structure-activity relationships (SARs) and facilitates optimization of the biological properties of candidate molecules. One of the most Dynamics areas of research is the development of new therapies for chronic metabolic diseases, particularly diabetes mellitus. Diabetes is a complex pathology marked by abnormal regulation of glucose homeostasis. This can result from either absolute insulin deficiency (type 1 diabetes) or peripheral insulin resistance, often associated with insufficient secretion (type 2 diabetes). This disease is associated with major systemic complications, including nephropathy, retinopathy, peripheral neuropathy, and cardiovascular disease, making it a global therapeutic challenge [1,2].

In the pursuit of new pharmacologically active entities, researchers are turning to simple, scalable, and chemically reactive aromatic motifs, such as 2-nitroaniline. This aromatic molecule, derived from aniline, consists of a benzene ring substituted with an amino group (-NH₂) in position 1 and a nitro group (-NO₂) in position 2. This particular configuration leads to significant intramolecular electronic interactions, including mesomeric and inductive effects, as well as intramolecular hydrogen bonding. These interactions modify not only the chemical reactivity of the molecule, but also its behavior as a potential ligand for biological targets. It has been determined that a significant number of 2-nitroaniline derivatives function as enzyme inhibitors, allosteric modulators, or precursors of pharmacophore structures [3].

A key aspect of its chemical reactivity is the regioselectivity of aromatic electrophilic or nucleophilic substitution reactions on the benzene ring. This regioselectivity is derived directly from the electron density distribution on the molecule. This distribution is influenced by the functional groups and their relative positions. To rationalize this selectivity, theoretical chemistry employs several predictive tools, including molecular electrostatic potential (MEP/ESP), Fukui indices (f^+ , f^- , f^- , g^-), and concepts from HSAB (Hard and Soft Acids and Bases) theory. These indicators can be used to identify the most reactive nucleophilic and electrophilic sites, based on charge distribution and transition state stability [4].

Once promising 2-nitroaniline derivatives have been identified, a crucial step is to predict their ability to interact with specific biological targets. In such cases, molecular docking is a valuable tool. This is a three-dimensional modeling technique that simulates the insertion of a ligand into the active site of a macromolecule, such as an enzyme (DPP-4, α -glucosidase) or a nuclear receptor (PPAR γ , among others). This approach enables the assessment of binding energies, the visualization of stabilizing non-covalent interactions (hydrogen bonds, π - π interactions, salt bridges), and the execution of virtual screening of compound libraries. This approach has the potential to significantly reduce the cost and duration of the drug discovery process [5].

The study of 2-nitroaniline and its derivatives demonstrates the efficacy of an integrated approach, combining organic chemistry, theoretical chemistry, and molecular pharmacology, to design new therapeutic agents. This multidisciplinary approach is crucial to address current medical challenges, especially in the context of complex chronic diseases like diabetes [6].

SIRT6 is a histone H3 deacetylase, and its inhibitors have been considered as potential agents for the treatment of diabetes. Weining Sun and his team have synthesized a series of new SIRT6 inhibitors that contain the squelette 1-phenylpiperrazine [7]. The antidiabetic properties of these compounds have been studied. The results showed that 5-(4-methylpiperazin-1-yl)-2-nitroaniline is the most potent inhibitor of SIRT6.

Our study is structured around two parts. In the first part, a theoretical study was conducted on the regeoselectivity of the transetherification reaction of 4,5-dialkoxy-2-nitroanilines. This study is based on the reactivity descriptors and concepts derived from the DFT approach.

In the second part, we carried out, *in silico* study of the antidiabetic properties of 5-(4-methylpiperazin-1-yl)-2-nitroaniline and its analogs. Several computational chemistry methods have been used, including molecular docking, molecular Dynamics, bioisosteric replacement, and ADME property prediction.

This manuscript is structured into three chapters:

Chapter 1: This chapter provides a bibliographic overview of diabetes and nitroaniline compounds.

Chapter 2: This chapter focuses on the theoretical study on the regional study of the transetherification of 4,5-dialkoxy-2-nitroanilines.

Chapter 3: In this chapter, we will use *in silico* analyses to gain a better understanding of the binding mechanism and intermolecular interactions of 5-(4-methylpiperazin-1-yl)-2-nitroaniline and its analogs with the SIRT6 receptor.

References

- [1] D. Leroith, S.I. Taylor, J.M.Olefsky, Diabetes Mellitus: A Fundamental and Clinical Text, Lippincott Williams & Wilkins, USA, 2004.
- [2] World Health Organization (WHO) Diabetes. https://www.who.int/news-room/fact sheets/detail/diabetes.
- [3] Z. Rappoport, The Chemistry of Anilines, Part 1, John Wiley & Sons, Ltd., 2007.
- [4] H.C. Da Silva, T. Leite, S.C. Rodrigues, B.L.C. De Carvalho, M.T. Martins, R.G. Fiorot, F.R.F. Dias, Theoretical Investigation of Regiodivergent Addition of Anilines and Phenolates to Benzoquinone Derivatives, ACS Omega, 7(44), 2022.
- [5] R. Baron, Computational Drug Discovery and Design, Humana Press Inc., New Jersey, 2016.
- [6] D.B. Kitchen, H. Decornez, J.R. Furr, J. Bajorath, Docking and scoring in virtual screening for drug discovery: methods and application, Nature reviews Drug discovery, 2004, 3(11):935-49.
- [7] W. Sun, X. Chen, S. Huang, W. Li, C Tian, S. Yang, L. Li, Discovery of 5-(4-methylpiperazin-1-yl)-2-nitroaniline derivatives as a newclass of SIRT6 inhibitors, Bioorganic & medicinal chemistry letters, 2020,30, 127215.

Chapter	<i>I</i> :
1	

Overview of Diabetes and Nitroaniline Compounds

Part 1: Overview of diabetes

I.1.1. Introduction

Today, diabetes mellitus is one of the most widespread and worrying chronic diseases worldwide. Growing rapidly, particularly in middle-income countries, this disease is no longer confined to medical issues, but now extends to social, economic and pharmaceutical considerations. According to data from the World Health Organization, diabetes affects more than 500 million people worldwide, a figure that is constantly rising, heralding a veritable silent pandemic [1-2].

This pathology results from a complex imbalance involving carbohydrate metabolism, pancreatic function and cellular insulin signalling. Much more than a simple blood sugar disorder, diabetes is a major risk factor for cardiovascular disease, end-stage renal failure, peripheral neuropathy and blindness. These complications, heavy in terms of morbidity and healthcare costs, confirm the urgent need to reinforce prevention strategies and therapeutic innovation [3].

In this context, the pharmaceutical industry plays a central role. The development of new molecules, the search for specific biological targets, as well as the optimization of galenic forms and administration devices represent major areas of research. From metformin and SGLT2 inhibitors to GLP-1 analogs, the pharmaceutical industry has a key role to play in this area. Pharmaceutical advances have transformed the management of diabetes over the past two decades [4].

This chapter takes an in-depth look at the pharmaceutical dimension of diabetes, highlighting the disease's pathophysiological mechanisms, the major therapeutic classes available, and the innovations emerging from modern pharmaceutical research. The aim is to understand the scientific, industrial and clinical challenges raised by the fight against this multifaceted pathology [5].

I.1.2 Diabetes definition

Diabetes is a chronic disease that occurs either when the pancreas does not produce enough insulin or when the body cannot effectively use the insulin it produces. Insulin is a hormone that regulates blood glucose. Hyperglycaemia, also called raised blood glucose or raised blood sugar, is a common effect of uncontrolled diabetes and over time leads to serious damage to many of the body's systems, especially the nerves and blood vessels.

In 2022, 14% of adults aged 18 years and older were living with diabetes, an increase from 7% in 1990. More than half (59%) of adults aged 30 years and over living with diabetes were not taking medication for their diabetes in 2022. Diabetes treatment coverage was lowest in low- and middle-income countries.

In 2021, diabetes was the direct cause of 1.6 million deaths and 47% of all deaths due to diabetes occurred before the age of 70 years. Another 530 000 kidney disease deaths were caused by diabetes, and high blood glucose causes around 11% of cardiovascular deaths.

Since 2000, mortality rates from diabetes have been increasing. By contrast, the probability of dying from any one of the four main noncommunicable diseases (cardiovascular diseases, cancer, chronic respiratory diseases or diabetes) between the ages of 30 and 70 decreased by 20% globally between 2000 and 2019 [6].

I.1.3. Classification and pathophysiology

Diabetes is a heterogeneous complex metabolic disorder characterized by elevated blood glucose concentration secondary to either resistance to the action of insulin, insufficient insulin secretion, or both. The major clinical manifestation of the diabetic state is hyperglycemia. However, insulin deficiency and/or insulin resistance also are associated with abnormalities in lipid and protein metabolism, and with mineral and electrolyte disturbances. The vast majority of diabetic patients are classified into one of two broad categories: type 1 diabetes mellitus, which is caused by an absolute or near absolute deficiency of insulin, or type 2 diabetes mellitus, which is characterized by the presence of insulin resistance with an inadequate compensatory increase in insulin secretion (Figure I.1). In addition, women who develop diabetes during their pregnancy are classified as having gestational diabetes. Finally, there are a variety of uncommon and diverse types of diabetes, which are caused by infections, drugs, endocrinopathies, pancreatic destruction, and genetic defects. These

unrelated forms of diabetes are included in the "Other Specific Types" and classified separately [7-8].

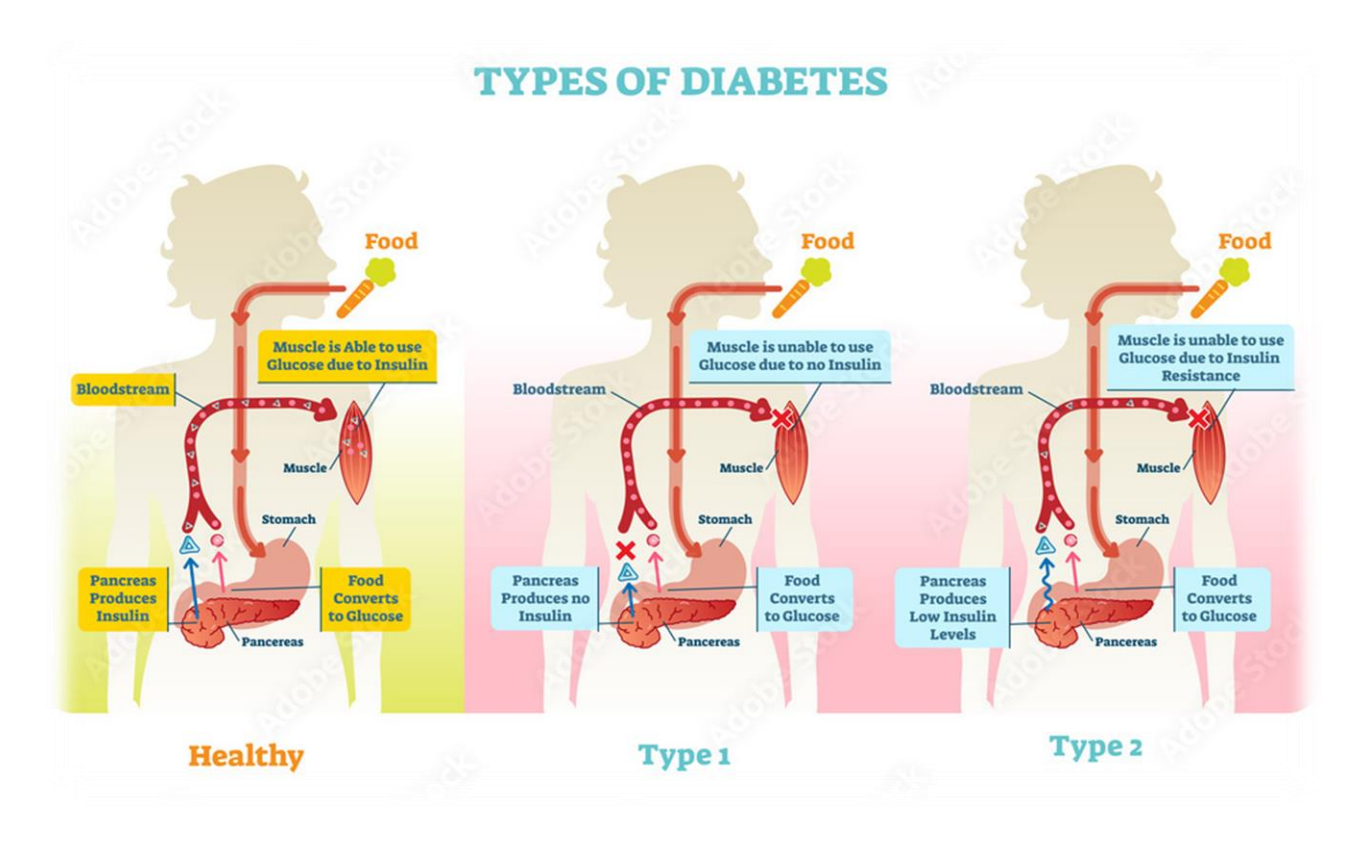


Figure I. 1: Types of diabetes vector illustration diagram scheme

I.1.4. Diagnosis and treatment

Early diagnosis can be accomplished through relatively inexpensive testing of blood glucose. People with type 1 diabetes need insulin injections for survival. One of the most important ways to treat diabetes is to keep a healthy lifestyle. Some people with type 2 diabetes will need to take medicines to help manage their blood sugar levels. These can include insulin injections or other medicines. Some examples include:

- metformin
- sulfonylureas
- sodium-glucose co-transporters type 2 (SGLT-2) inhibitors.

Along with medicines to lower blood sugar, people with diabetes often need medications to lower their blood pressure and statins to reduce the risk of complications (Figure I.2).

Additional medical care may be needed to treat the effects of diabetes:[9]

- foot care to treatuleers
- screening and treatment for kidney disease
- eye exams to screen for retinopathy (which causes blindness).

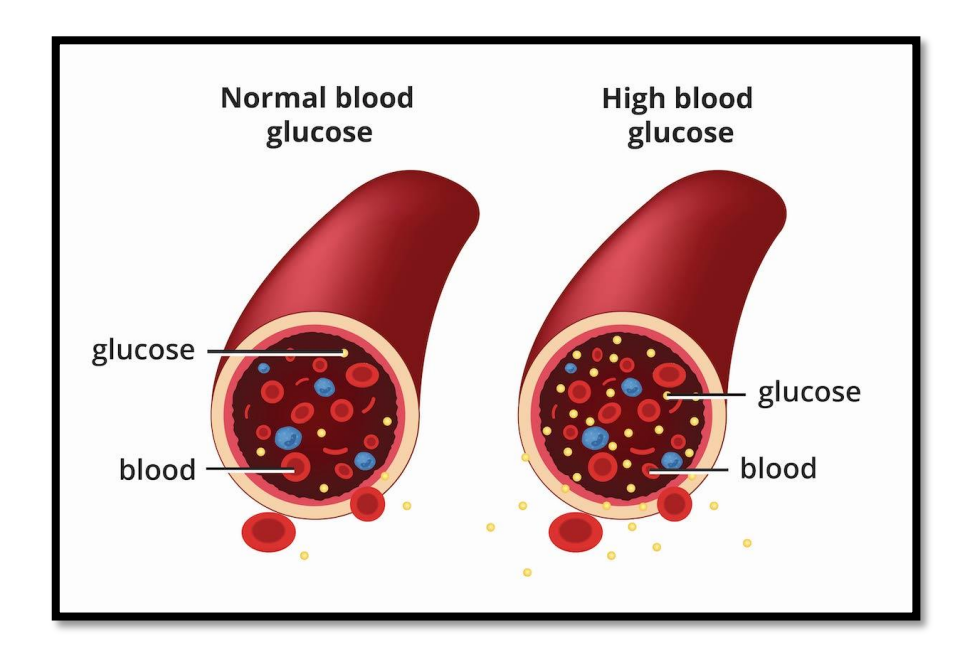


Figure I. 2: High blood glucose normal glucose design vector illustration.

I.1.5. Pharmaceutical research and innovation

Advances in pharmaceutical research have enabled the development of drugs targeting more specific mechanisms. Molecular modeling techniques, such as molecular docking, are used to identify new compounds active against targets such as the DPP-4 enzyme or the GLP-1 receptor. These methods can predict the binding affinity between drug candidates and their biological targets, accelerating the discovery of new therapies [10].

Part 2: Overview of Nitroaniline Compounds

I.2.1. Definition

Nitroanilines are a family of aromatic organic compounds derived from aniline in which a hydrogen atom on the benzene ring is replaced by a nitro group (-NO₂). Thus, the molecule has both an amino group (-NH₂) and a nitro group attached to a benzene ring, making them substituted aromatic amines. There are three nitroaniline isomers that differ in the relative position of the functional groups: 2-nitroaniline (ortho), 3-nitroaniline (meta), and 4-nitroaniline (para). This diversity of isomers influences their physical properties, chemical reactivity and industrial applications. These compounds are widely used as intermediates in the synthesis of dyes, pigments, pharmaceuticals, and agrochemicals.[11]

I.2.2. Nitroaniline - structure and molecular properties

2-Nitroaniline, also known as 2-nitrobenzenamine, is the ortho isomer of nitroaniline (Figure I.3). Its molecular formula is $C_6H_6N_2O_2$ and its molecular weight is approximately 138.13 g/mol. The molecule consists of a benzene ring with an amino group (-NH₂) in position 1 and a nitro group (-NO₂) in position 2. This particular spatial configuration allows the formation of intramolecular hydrogen bonds between the NH₂ and NO₂ groups, which has a significant impact on the physicochemical properties of the molecule, such as its solubility, polarity and thermal stability. The electronically contrasting character of these two functional groups (one electron donor, the other attractor) gives the molecule an asymmetric polarization of the aromatic π -system, which strongly influences its reactivity [12-13].

Figure I. 3: Structure of 2-Nitroaniline.

I.2.3. Physico-chemical properties

At room temperature, 2-nitroaniline is a pale yellow, crystalline, moderately volatile solid. It has a melting point between 71 and 74°C and is sparingly soluble in water but readily soluble in a number of organic solvents such as ethanol, acetone and chloroform. Due to its two polar groups, the molecule has a high polarity, making it suitable for use in a variety of reaction media. Spectroscopically, the molecule shows characteristic bands in IR (NO₂, NH₂ vibrations) and its electronic transitions can be observed in UV-visible due to its conjugated system [13].

I.2.4. Chemical reactivity

2-Nitroaniline is an important intermediate in many organic reactions. The amino group is a nucleophilic site that can undergo reactions such as acetylation, diazotization, or formation of azo bonds (in dye chemistry). The nitro group, on the other hand, can be reduced to an amine group, giving rise to diamines used in polymer synthesis. The proximity of the two groups (ortho) also influences the reaction mechanisms, especially in aromatic electrophilic substitution, where the reactivity of the ring is modified by antagonistic mesomeric and inductive effects. Because of this duality, 2-nitroaniline has been widely studied in theoretical chemistry, especially in the analysis of charge distribution, molecular electrostatic potential (MEP) or local reactivity (Fukui indices) [14-15].

I.2.5. Toxicity and safety

2-Nitroaniline is classified as a human toxicant. It can be absorbed through the skin, respiratory tract, or gastrointestinal tract. Prolonged or excessive exposure may cause skin irritation, respiratory problems, or even methemoglobinemia, a blood disorder that affects the ability to carry oxygen. In addition, certain nitroaniline derivatives have been identified as potential mutagens or carcinogens. For this reason, nitroaniline must be handled in the laboratory under a fume hood, with gloves, goggles, and appropriate protective equipment. Waste should be handled in accordance with hazardous chemical management protocols [13].

I.2.6. Industrial and scientific applications

2-Nitroaniline plays an essential role as a precursor in the production of azo dyes, which are widely used in inks, textiles and plastics. It is also used in the manufacture of pharmaceutical products, particularly in the synthesis of anti-inflammatory, antimicrobial and anticancer molecules. In materials chemistry, its derivatives are sometimes incorporated into

functional polymers or electro-optical materials. In fundamental research, it is studied for its electronic and spectroscopic properties and serves as a model molecule in quantum chemical calculations and orbital reactivity analyses [16].

I.2.7. Aromatic substitution reactions

Substitution reactions on aromatic rings are central to organic chemistry. Besides the commonly encountered electrophilic aromatic substitution [17], other mechanisms include SNAr nucleophilic aromatic substitutions [18] and the distinct but related SNArH and vicarious nucleophilic substitutions [19], substitutions brought about through benzyne intermediates, [20-21] radical mechanisms including electron transfer-based SRN1 reactions [22] and base-promoted homolytic aromatic substitution (BHAS) couplings, sigma tropic rearrangements, substitutions arising from deprotonation of arenes (directed metalations), the vast array of organometallic mechanisms and SN1 reactions. All of these areas of chemistry are too vast to reference comprehensively, and so are simply represented here by one or two key reviews or recent references. Among these various reaction types, SNAr reactions have attracted a lot of recent attention, because of a recognition that many such reactions may proceed by concerted (cSNAr) [23], rather than classical two-step mechanisms.

I.2.8. Classical nucleophilic aromatic substitution

Nucleophilic aromatic substitutions have been studied at least since the 1870s. The long-accepted mechanism [19-20], exemplified in Figure I.4 for dinitroarene 1, involved a two-stage process that featured a Meisenheimer intermediate 2. In these substitutions, the arene is significantly activated for substitution by the presence of one or more electron-withdrawing substituents in the positions that are ortho or para to the site of substitution to provide resonance stabilisation, and with nitro as a favoured substituent. In Terrier's excellent book on SNAr reactions in 2013 [18], he wrote that 'concerted reactions are the exception rather than the rule' and 'there is little doubt that most of the activated SNAr substitutions must proceed through the early-recognised addition-elimination mechanism'.

Figure I. 4 : Classical two-step mechanism for SNAr reactions.

Evidence in favour of a two-stage substitution was cited when intermediates were isolated. Thus, as reviewed by Bunnett and Zahler [17] in 1951, a number of reactions gave rise to isolated intermediate adducts as shown in FigureI.3 Key studies were performed by Meisenheimer, who isolated a common intermediate 5 from reaction of methyl ether 4 with NaOEt, and from reaction of NaOMe with the ethyl ether 6.

OME O₂N
$$\rightarrow$$
 NO₂ \rightarrow N

Figure I. 5 : Some known Meisenheimer intermediates.

I.2.9. Mechanism of nucleophilic aromatic substitution

The first step is attack of the nucleophile on the electron-poor ring to generate a negatively charged intermediate (e.g., the "Meisenheimer" intermediate, above) [24].

Since this disrupts the aromaticity of the ring, it's also the rate-limiting step:

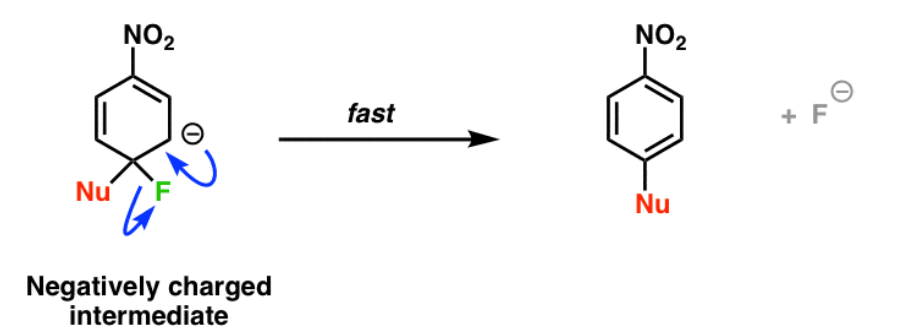
➤ first step: attack of electron-poor aromatic ring by nucleophile, forming a negatively charged intermediate.

12 | Page

In electrophilic aromatic substitution (EAS) we saw that electron-rich substituents stabilized the electron-poor intermediate.

But in nucleophilic aromatic substitution (NAS) the tables are turned! Instead, the intermediate is electron-rich, and is stabilized by electron-withdrawing substituents, such as NO₂.

> The second step (fast) in nucleophilic aromatic substitution is expulsion of the leaving group:



References

- [1] Organisation Mondiale de la Santé (OMS). Diabète. https://www.who.int/fr/news-room/fact-sheets/detail/diabetes
- [2] American Diabetes Association (ADA). Standards of Medical Care in Diabetes 2024. https://professional.diabetes.org/standards-of-care
- [3] Nathan DM. Diabetes: Advances in Diagnosis and Treatment.JAMA, 2015, 314 (10):1052–1062.
- [4] Bailey CJ, Day C. Traditional therapies for diabetes. British Medical Journal (BMJ).2019.
- [5] Baron R (Ed). Computational Drug Discovery and Design. Methods in Molecular Biology, vol. 1520, Springer, 2017.
- [6] Global Burden of Disease Collaborative Network. Global Burden of Disease Study 2021. Results. Institute for Health Metrics and Evaluation. 2024
- [7] Classification and Diagnosis of Diabetes Mellitus: Standards of Medical Care in Diabetes. Diabetes Care 41 (Suppl 1): S13-S27, 2018.
- [8] MellitusCarolina Solis-Herrera, MD, Curtis Triplitt, PharmD, Charles Reasner, M.D.+, Ralph A DeFronzo, M.D., and Eugenio Cersosimo, M.D.Classification ofDiabetes, PhD.February 24, 2018.
- [9] Diabetes, Peer reviewed by Dr Rosalyn Adleman, MRCGPLast updated by Dr Doug McKechnie, MRCGP, 4 Mar 2025
- [10] Riccardo Baron, Computational Drug Discovery and Design, Book,2012.
- [11] P. C. Chen, W. Lo & K. H. Hu, Molecular structures of mononitroanilines and their thermal decomposition products, pages 99–112, (1997).
- [12] PubChem CID 10467 2-Nitroaniline: https://pubchem.ncbi.nlm.nih.gov/compound/2-Nitroaniline.
- [13] Sigma-Aldrich Product Sheet for 2-Nitroaniline: https://www.sigmaaldrich.com
- [14] Domingo, L. R., et al. (2002). "Quantitative characterization of the local electrophilicity of organic molecules." J. Org. Chem. 67, 8911–8919.
- [15] Parr, R. G., & Yang, W. (1989). Density-Functional Theory of Atoms and Molecules, Oxford University Press.
- [16] I. Din, R. Khalida, Z. Hussaina, J. Najeeb, A. Sahrifa, A. Intisar and E. Ahmeda, Critical review on the chemical reduction of nitroaniline, RSC Advances, 32, 2020, 10, 19041-19058.
- [17] M. B. Smyth, in MarchQs Advanced Organic Chemistry: Reactions, Mechanisms and Structure, 7th ed., Chap. 11, pp. 569–641, e-book ISBN: 9781118472217. Wiley, Hoboken, 2013.

- [18] J. F. Bunnett, R. E. Zahler, Chem. Rev. 1951, 49, 273 –412.
- [19] K.Błaziak, W. Danikiewicz, M. Ma kosza, J. Am. Chem. Soc.2016, 138, 7276–7281, and references therein.
- [20] H.Takikawa, A. Nishii, T. Sakai, K. Suzuki, Chem. Soc. Rev. 2018, 47, 8030–8056.
- [21] J. A. Garcia-Llpez, M. F. Greaney, Chem. Soc. Rev. 2016, 45,6766–6798.
- [22] R. A. Rossi, A. B. Pierini, A. B. PeÇeÇory, Chem. Rev. 2003,103, 71–168.
- [23] E. E. Kwan, Y. Zeng, H. A. Besser, E. N. Jacobsen, Nat. Chem. 2018, 10, 917 923.
- [24] J. Ashenhurst, Reactions of Aromatic Molecules, https://www.masterorganicchemistry.com/2018/08/20/nucleophilic-aromatic-substitution-nas/

Chapter II:

Theoretical Study on the Regioselectivity of the Transetherification of 4,5-Dialkoxy-2-nitroaniline

II.1. Introduction

4,5-Dialkoxy-2-nitroaniline with two different alkoxy chains are precursors for the synthesis of several primaquine derivatives and other heterocyclic compounds. These compounds exhibit important antimalarial properties [1].

Regioselectivity is an important characteristic, especially when one of the reaction products is a major regioisomer. Therefore, it is essential to comprehend the factors inducing the different types of selectivity in order to rationalize them.

According to recent research by Jarosław Grolikand al. [2], these compounds exhibit high regioselectivity in transetherification reactions (Figure II.1).

Furthermore, in order to comprehend and rationalize of the reactive processes that are a part of organic chemistry, theoretical chemists have devoted considerable effort to developing theories and computational principles.

In recent years, reactivity descriptors derived from conceptual DFT have been widely used [3], particularly in organic chemistry, to identify reactive sites and thus determine the reactivities of molecules with each other.

Chemical reactivity relies mainly on global descriptors derived from electronic properties, while selectivity relies more on local quantities. The Fukui function is by far the most important local reactivity descriptor.

The theoretical investigation of the regioselectivity of the aromatic nucleophilic substitution (ArSN) reaction on 4,5-dialkoxy-2-nitroanilines is the main topic of this chapter.

Our research focuses mainly on studying the regioselectivity of two nucleophilic attack sites: C4 and C5 atoms.

We used a Density Functional Theory (DFT) approach, to compute the local and global indices, Fukui indices, and molecular electrostatic potential (MEP) mapping, aiming for a comprehensive analysis of the selectivity region in this reaction.

Figure II. 1: Transetherification reactions of 2-nitroanilines

We chose a series of 4,5-dialkoxy-2-nitroanilines (Table II.1) to investigate the impacts of electronic effects (donor and acceptor) of alkoxy groups on the regionselectivity of the transetherification reaction.

Table II. 1: Chemical structure 4,5-dialkoxy-2-nitroanilines under study

Comp.	R1	Comp.	R1
1	CH(CH ₃)Cl	4	CH ₃
2	C(CH ₃)Cl ₂	5	CH(CH ₃) ₂
3	CCl ₃	6	$C(CH_3)_3$

II.2. Computational methods:

All the calculations were performed with the Gaussian 09 package [5]. Full geometry optimization was carried out at the DFT [6] method by employing Becke's three-parameter hybrid functional (B3LYP) [7,8] and 6–311++G(d,p) basis set. The atomic charges have been assessed using the Hirshfeld electronic population analysis (HPA) [9].

The molecular geometries have been optimized in ethanol as implicit solvent using the C-PCM solvation model [10].

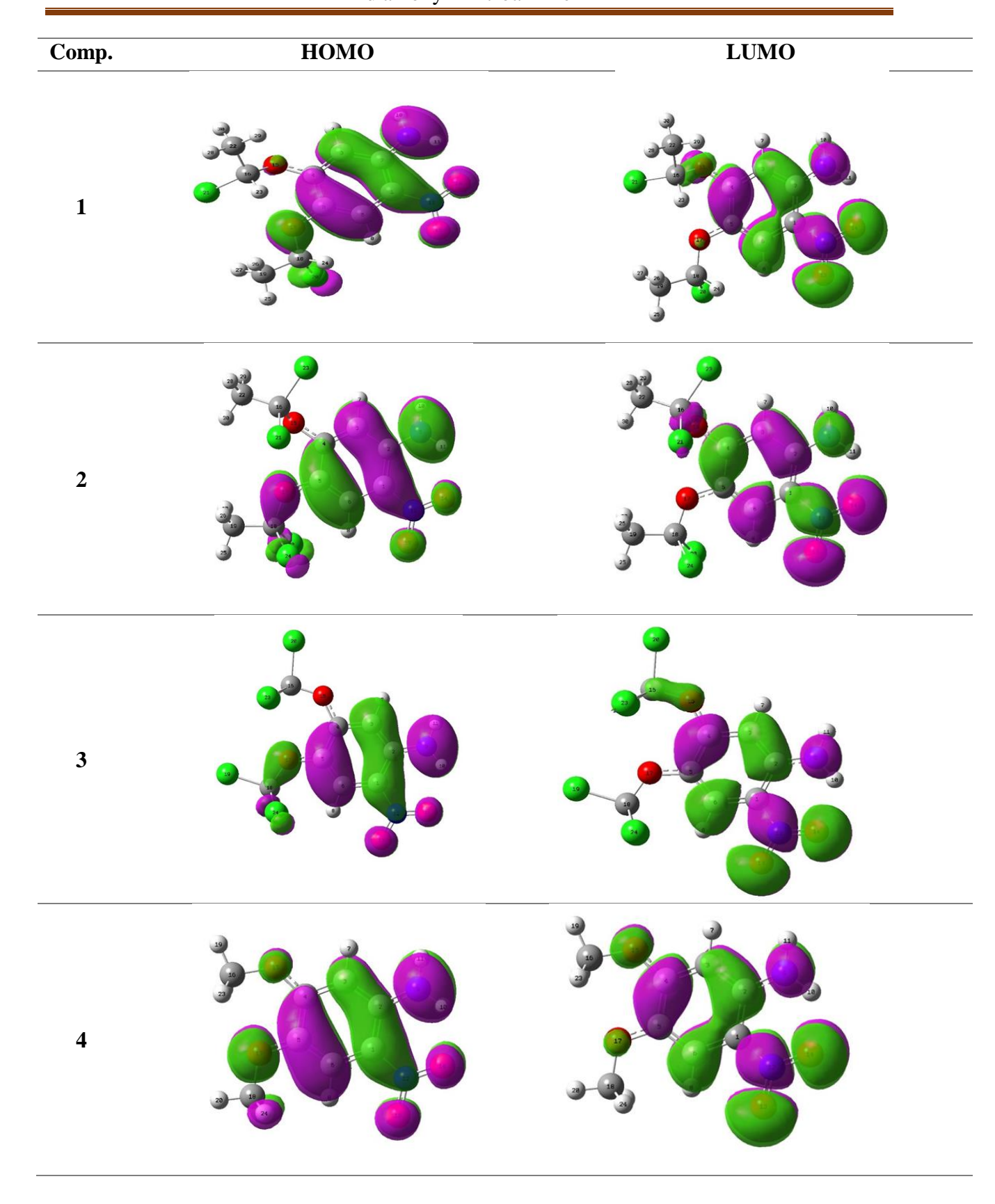
This work also includes calculation of 3D MESP surface map and 2D MESP contour map to reveal the information regarding charge transfer within the molecule [11].

II.3. Frontier molecular orbitals (HOMO and LUMO)

Frontier molecular orbitals, namely the lowest unoccupied molecular orbital (LUMO) and the highest occupied molecular orbital (HOMO), are essential orbitals playing a critical role in chemical stability and reactivity [12].

The contour plots of the frontier molecular orbitals (LUMO and HOMO) of all molecules are shown in Figure II.2.

LUMO orbitals are more widely localized on the C4 atom than on the C5 atom. This result indicates that this atom is the preferred site for nucleophilic attack.



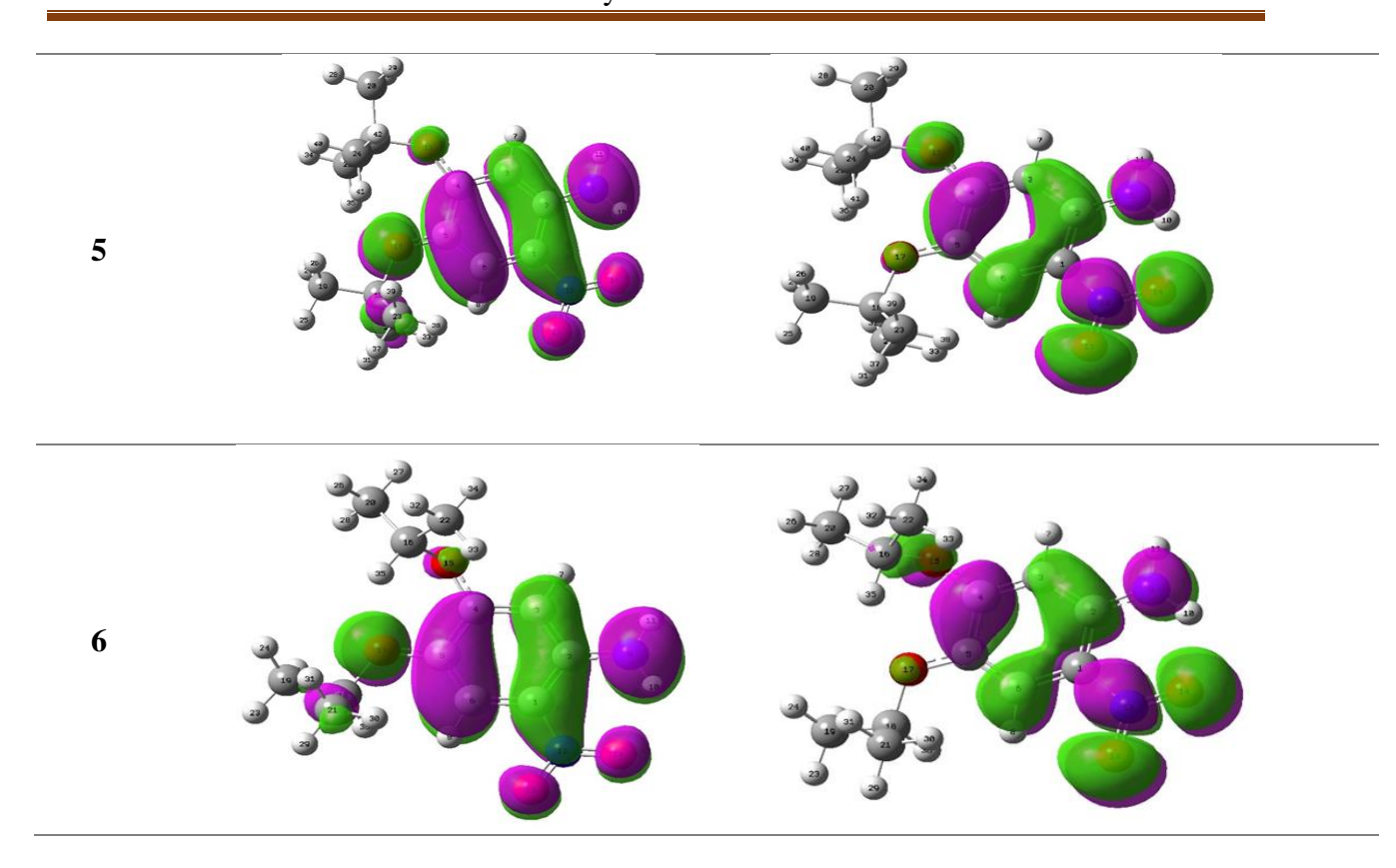


Figure II. 2: Frontier molecular orbitals plots of 4,5-Dialkoxy-2-nitroanilines

II.4. Global and local reactivity descriptors

II.4.1. Global HSAB (Hard and Soft Acids and Bases) principle II.4.1.1. Definitions

The hard/soft acid-base principle has long been known to be an excellent predictor of chemical reactivity [13].

Hard and soft acids and bases were initially defined as follows:

- a) *Soft base*: characterized by a donor atom with high polarizability, low electronegativity oxidizable and associated with low empty orbitals.
- b) *Hard base*: characterized by a donor atom with low polarizability, high electronegativity, difficult to reduce and associated with empty orbitals with high energies and therefore inaccessible.
- c) *Soft acid*: characterized by an acceptor atom with a low positive charge, a large size. It has several easily excitable external electrons and is polarizable.
- d) *Hard acid:* characterized by an acceptor atom with a large positive charge and a smallsize. It has no easily excitable external electrons and is non polarizable. These

qualitative definitions enable us to place acids and bases in one of two 'boxes' called 'hard' and 'soft', but without any classification.

II.4.1.2. Statement of the HSAB principle

Given an acid-base equilibrium:

$$A +: B \leftrightarrow A - B$$

Where A is a Lewis acid (electron acceptor) and B is a Lewis base (electron donor). Based on various experimental data [14-16], Pearson presented a classification of Lewis acids into two groups (a) and (b), taking as his starting point the starting point taking as a starting point of the Lewis base donor atoms according to increasing electronegativity:

$$As < P < Se < S < I < C < Br < Cl < N < O < F$$
 (series *)

The criterion used is that Lewis acids in group (a) will form more stable complexes with donor atoms of higher electronegativity (right of series*); whereas Lewis acids of group (b) will react preferentially react with donor atoms with low electronegativity (left of series *).

Based on this distribution, Pearson noted that acids in group (a)have small, positively charged acceptor atoms (H⁺, Li⁺, Na⁺, Mg2⁺, etc.);

While acids in group (b) have acceptor atoms with low positive charges positive charges and larger sizes (Cs⁺, Cu⁺, etc.).

 Table II. 2: Hard/Soft characteristics in HSAB principle.

HSAB principle	Hard	Soft		
	- Strong positive charge	-Low positive charge		
Acid	- Low polarizability	-High polarizability		
	- Small size	-high size		
Base	-High electronegativity -Difficult to oxidize -Low polarizability	-Low electronegativity -Easily oxidized -High polarizability		

II.4.2. Chemical concepts and reactivity indices derived from DFT

II.4.2.1. Global Indices derived from conceptual DFT

Density Functional Theory (DFT) has seen significant development in recent years. This approach treats the ground-state energy of a system as a functional of a three-dimensional electron density. The application of the variational principle leads to the Kohn-Sham equations, which are similar to the Hartree-Fock equations. Essentially, the exchange contribution in the Fock operator is replaced by an exchange-correlation potential, derived from the functional of exchange and correlation energy with respect to electron density.

A key challenge in DFT is that the exact exchange-correlation energy is not known. However, approximate formulas for this energy produce results comparable to or better than MP2 methods, with lower computational costs. Early DFT approximations mirror those of HF methods. The Schrödinger equation used is time-independent and non-relativistic. From the Born-Oppenheimer approximation, the formalisms and approximations diverge [6]. Currently, DFT provides a valuable framework for chemical concepts such as electronic chemical potential, electronegativity, hardness, softness, electrophilicity, and more. DFT is based on the variational principle, asserting that a system's energy is a functional of its electron density:

$$E = E[\rho]$$

To obtain the optimal density, the energy E is minimized, subject to the constraint:

$$\int \rho(\mathbf{r}) d\mathbf{r} = \mathbf{N}$$

Using the method of Lagrange multipliers, this constraint leads to the following variational condition:

$$\delta[E - \mu \rho] = 0$$

Where μ is the Lagrange multiplier, also defined as the electronic chemical potential according to Parr:

$$\mu = (\partial E / \partial N)v(r) = -\chi$$

The connection with classical chemistry is achieved with the identification of μ as the negative of electronegativity χ .

a) Electronic Chemical Potential

The Lagrange multiplier μ corresponds to the electronic chemical potential, aligning with Pearson's definition. It describes the tendency of electrons to escape from the system, indicating the flow direction of electron density during a chemical reaction [6].

b) Global Hardness and Softness

The fundamental DFT expression for energy variation from one stationary state to another is:

$$dE = \mu dN + \int \rho(r) dv(r) dr$$

where:

- μ is the chemical potential,
- $\rho(r)$ is the electron density,
- v(r) is the system's external potential.

The first derivative of μ with respect to N (the total number of electrons) defines the global hardness η , while the reciprocal, S, represents the global softness [17]:

$$\eta = (\partial \mu \, / \, \partial N) v(r)$$

$$S = 1/2 \eta$$

Electronic chemical potential μ and global hardness η can be approximated using the frontier molecular orbital energies ϵ_{HOMO} and $\epsilon_{LUMO}[18-19]$:

$$\mu = (\epsilon_{\text{HOMO}} + \epsilon_{\text{LUMO}}) / 2$$

$$\eta = \epsilon_{LUMO} - \epsilon_{HOMO}$$

c) Global Electrophilicity Index

The electrophilicity index ω , linked to the chemical potential μ , is given by [18]:

$$\omega = \mu^2 / 2\eta$$

This index measures an electrophile's ability to acquire additional electronic charge.

d) Global Nucleophilicity Index

Unlike electrophilicity, nucleophilicity cannot be defined through a variational procedure since removing electron density does not stabilize a molecule. Domingo et al. proposed that

low electrophilicity often implies high nucleophilicity for simple molecules [19]. However, this inverse relationship does not hold for complex molecules with multiple functional groups, like donor-acceptor ethylenes (CD ethylenes), which can be both good nucleophiles and electrophiles.

Therefore, nucleophilicity cannot simply be defined as the inverse of electrophilicity. Domingo et al. recently showed that nucleophilicity relates to a molecule's ability to release electron density. The simplest approach considers nucleophilicity as the negative value of gasphase ionization potential (IP):

$$N = -IP$$

Higher nucleophilicity corresponds to lower ionization potentials and vice versa. Domingo et al. [20] also introduced an empirical nucleophilicity index (N) based on Kohn-Sham HOMO energies, relative to the tetracyanoethylene (TCE) molecule - a standard reference due to its extremely low HOMO energy.

The global reactivity indices derived from the conceptual-DFT such as: electronegativity (χ) , global hardness (η) , global softness (S), electrophilicity (ω) and nucleophilicity (N) are calculated and discussed to explain the global changes between the six 4,5-dialkoxy-2-nitroanilines. The results are summarized in Table II.3.

Table II. 3 : Values of HOMO-LUMO gap (Δ), global reactivity indices (χ , η , S, ω , N), and dipole moment (DM).

Comp.	E _{HOMO} (eV)	E _{LUMO} (eV)	Δ (eV)	χ (eV)	η (eV)	S (eV ⁻¹)	ω (eV)	N (eV)	DM (Dahya)
	(ev)	(0)	(ev)	(0)	(0)	(ev)	(0)	(0)	(Debye)
1	-6,29	-2,90	3,39	4,60	1,70	0,29	6,23	2,78	8.46
2	-6,46	-3,04	3,42	4,75	1,71	0,29	6,60	2,61	8.25
3	-6,64	-3,11	3,52	4,88	1,77	0,28	6,73	2,43	5.96
4	-5,95	-2,67	3,27	4,31	1,64	0,30	5,66	3,12	7.80
5	-5,82	-2,62	3,20	4,22	1,60	0,31	5,57	3,25	8.92
6	-5,91	-2,73	3,17	4,32	1,59	0,31	5,87	3,16	7.16

 $\Delta = \mid E_{HOMO} - E_{LUMO} \mid ; \chi = -\mu = 1/2 (A+I) ; \\ \eta = 1/2 (\eta = E_{LUMO} - E_{HOMO}) ; \\ S = 1/2 \eta ; \\ \omega = \mu^2/2 \eta ; \\ N = E_{HOMO} - E_{HOMO} (TCE) \\ with \\ E_{HOMO} (TCE) = -9.074535 \\ eV, \\ calculated \\ with DFT \\ B3LYP/6-311++G \\ (d,p) / \\ Hirshfeld/CPCM \\ model.$

The energy gap is the difference in energy between the HOMO and LUMO orbitals, which is an important parameter that can determine the reactivity or stability of molecules [9]. Table II.3 shows that 4,5-dialkoxy-2-nitroanilines with alkoxy groups that contain chlorine atoms (compounds 1, 2 and 3) are less reactive and more stable than those with methyl groups (compounds 4, 5 and 6). Compound 6 is the most reactive, has a lowest energy gap value (Δ = 3.17 eV).

Global softness (S) and global hardness (η) are two reactivity indices that show the chemical reactivity of the substance under study. A molecule with a smaller energy gap and low hardness can be classified as soft and chemically reactive. On the contrary, molecules with a larger energy gap (high η) can be considered as less reactive, hard, and kinetically stable.

The global hardness (η) of the studied compounds is classified from most reactive to least, as follows: compound 6, compound 5, compound 4, compound 1, compound 2 and compound 3 ($\eta = 1.59, 1.60, 1.64, 1.70, 1.71$ and 1.77 eV, respectively).

The global hardness results were validated by the HOMO-LUMO energy gap (Δ), which shows that low chemical reactivity (high η) is generally corresponds to to high kinetic stability (high Δ).

A good nucleophile is indicated by low values of electronegativity (χ), electrophilicity (ω) and high value of nucleophilicity (N). A good electrophile is indicated by high values of ω and χ (low value of N).

Compound 3 is the most electrophile, having the lowest nucleophilicity N (2,43 eV), the highest electronigativity (X = 4.88 eV), and the highest electrophilicity (ω = 6,73 eV).

Compound 5 is the most nucleophilic, as shown by its lowest electronigativity ($\chi = 4.22 \text{ eV}$), lowest electrophilicity ($\omega = 5.57 \text{ eV}$), and highest nucleophilicity N (3.25 eV).

The dipole moment values of all 4,5-dialkoxy-2-nitroanilines are higher than those of the simple 2-nitroaniline, which has a value of MD = 4.729 debye [21]. This can be explained by considering that 4,5-dialkoxy-2-nitroanilines have two methoxy groups, which increases their polarization.

II.4.2.2 Local reactivity indices derived from conceptual DFT

Chemists are mainly interested in the interactions between molecules, in other words, in chemical reactivity. To determine the reactive sites of a molecule in relation to an electrophile, nucleophile or radical, it is common to use net charges to favour one interaction over another. Nevertheless, it is well established that net charges calculated at the different

sites of a molecule are not always reliable descriptors of intermolecular interactions, particularly for reactions controlled by frontier orbitals, those governed by Soft-Soft interactions. Consequently, prediction of reactivity based solely on net charges can sometimes contradict experimental results [16-22].

To overcome these limitations, a more precise approach is to apply the HSAB principle at the local level, offering a better understanding of interactions between molecules. Local reactivity indices are particularly useful in this context [23]. In the following, we present the theoretical basis of the main local indices currently used to predict a molecule's reactive sites, in particular Fukui indices.

a) Fukui Indices

The Fukui function f_k , corresponding to the site k of a molecule, is defined as the first derivative of the electronic density $\rho(r)$ of a system with respect to the number of electrons N, at a constant external potential v(r): [24]

$$f_k = \left[\frac{\partial \rho(r)}{\partial N}\right]_{v(r)}$$

This function helps identify the regions of a molecule that are more likely to gain or lose electron density during a chemical reaction, providing insight into its reactive sites. The Fukui indices are crucial in predicting how a molecule will interact with electrophiles or nucleophiles, offering a more accurate and localized approach to chemical reactivity compared to net charges alone.

b) Condensed Form of Fukui Functions

The condensed form of Fukui functions for a molecule with N electrons was proposed by Yang and Mortier [25]. These indices help identify the most reactive sites of a molecule, depending on whether it undergoes a nucleophilic or electrophilic attack:

• For a nucleophilic attack (where the molecule accepts electrons):

$$f_k^+ = q_k(N+1) - q_k(N)$$

• For an electrophilic attack (where the molecule donates electrons):

$$f_k^- = q_k(N) - q_k(N-1)$$

Where:

• $q_k(N)$: Electronic population of atom k in the neutral molecule.

- $q_k(N+1)$: Electronic population of atom k in the anionic (N+1 electrons) molecule.
- $q_k(N-1)$: Electronic population of atom kin the cationic (N-1 electrons) molecule.

It has been shown that for frontier-controlled reactions, those driven by interactions between the HOMO and LUMO. A higher Fukui index value at a given site indicates greater reactivity of that site [26]. In other words:

- Sites with a high f_k^+ value are more susceptible to nucleophilic attack.
- Sites with a high f_k -value are more prone to electrophilic attack.

These indices provide a more precise, localized picture of a molecule's reactivity compared to global descriptors, making them a powerful tool in predicting reaction mechanisms.

In the transestherification reaction, the carbon atoms C4 and C5 in 2-nitoanilines are two sites of nucleophilic attack by the alkoxydes. The selectivity of atomic sites towards the approach of nucleophilic reactants is investigated using the condensed Fukui Functions $f^+(r)$ and dual descriptor $f^{(2)}(r)$. The numerical values of $f^+(r)$ and Hirshfeld atomic charge of C4 and C5 atoms are depicted in tables II.4. The dual descriptors $f^{(2)}(r)$ are mapped in figure II.3.

Table II. 4: Hirshfeld atomic charge Q and condensed Fukui functions $f^+(r)$ of the C4 and C5 atoms of 4,5-dialkoxy-2-nitroanilines under study.

Comp.	C	Q	<i>f</i> ⁺ (<i>r</i>)
1	C4	0.084	0.058
1	C5	0.051	0.031
2	C4	0.079	0.062
2	C5	0.051	0.031
3	C4	0.077	0.045
3	C5	0.039	0.020
4	C4	0.079	0.053
-	C5	0.050	0.032
5	C4	0.091	0.061
	C5	0.056	0.033
6	C4	0.079	0.059
U	C5	0.055	0.030

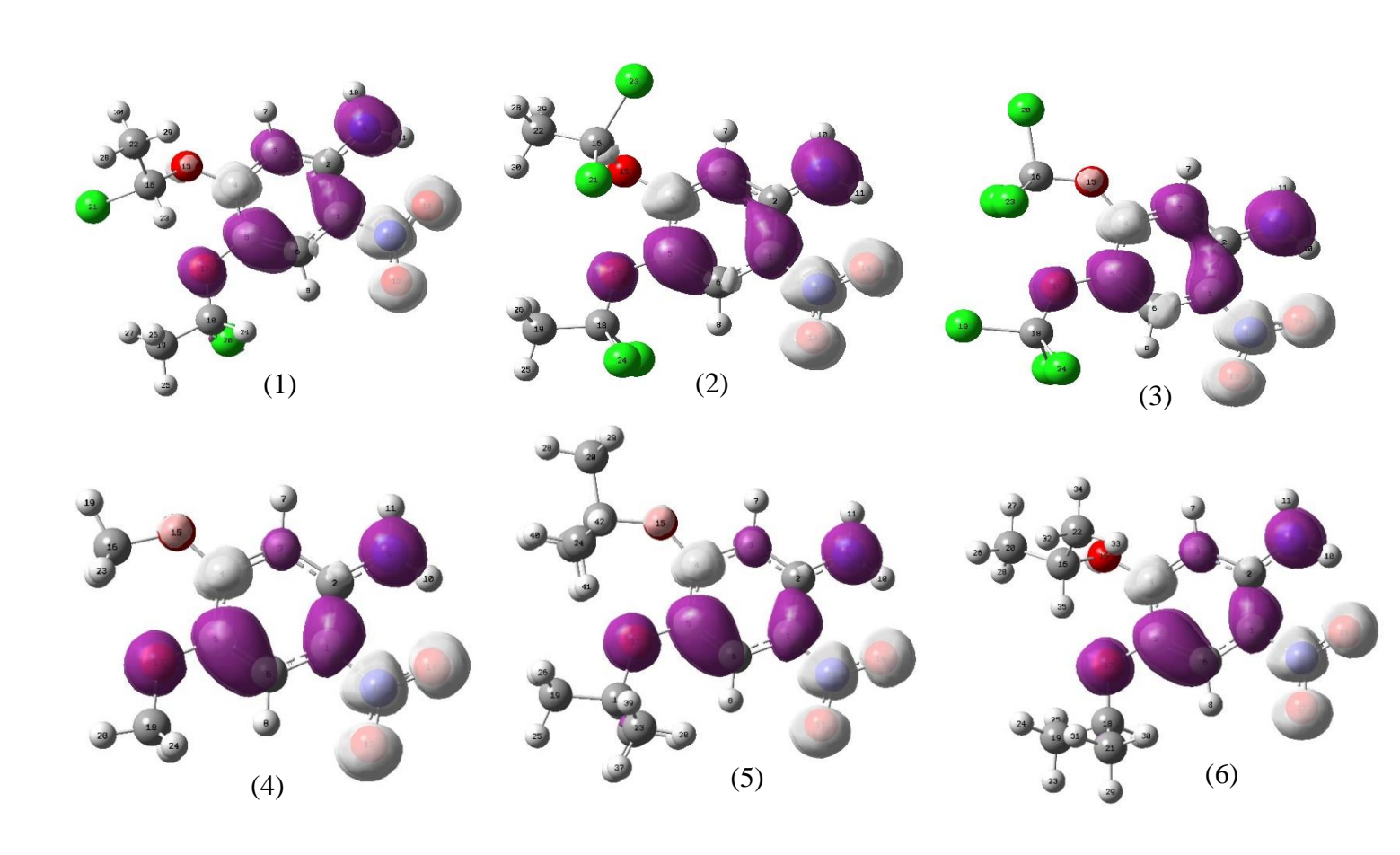


Figure II. 3: Dual descriptor 3D-mapped surfaces, mapped through (FMO) approximation, Isovalue MO = 0.0015 a.u, white color: regions of nucleophilic attacks, purple color: regions of electrophilic attacks.

Our results demonstrate that the $f^+(r)$ values of the C4 atom are higher than those of the C5 atom, confirming that C4 atom is a preferred site for nucleophilic attack (Table II.4). Furthermore, atomic charge calculations show that the C4 atom is significantly more electropositive than the C5 atom (Table II.4).

The selectivity of atomic sites toward the approach of nucleophilic reagents was also studied using the dual descriptor $f^{(2)}(\mathbf{r})$. The FMO approximation is used to map the dual descriptors $f^{(2)}(\mathbf{r})$ insurfaces. Local reactivity descriptors are shown in Figure II.3. Positive sign regions are shown in white, while negative sign regions are shown in purple (density = 0.00040 a.u., isovalue MO = 0.0015 a.u.). Our results show that the C4 atom is the preferred sites for nucleophilic attack.

II.5. Molecular Electrostatic Potential (MEP)

The molecular electrostatic potential (MEP) at a given point p(x,y,z) in the vicinity of a molecule is the force acting on a positive test charge (a proton) located at p through the electrical charge cloud generated through the molecules electrons and nuclei. Despite the fact that the molecular charge distribution remains unperturbed through the external test charge (no polarization occurs) the electrostatic potential of a molecule is still a good guide in assessing the molecules reactivity towards positively or negatively charged reactants. The MEP is typically visualized through mapping its values onto the surface reflecting the molecules boundaries. The latter can be generated through overlapping the VdW radii of all atoms of the molecule, through algorithms calculating the solvent accessible surface of the molecule, or through a constant value of electron density. These calculations allow us to visualize the most electronegative and electropositive regions of the molecule, indicating the most favorable sites for nucleophilic attack [27].

a) 3D-Molecular Electrostatic Potential

The molecular electrostatic potential surface is used to identify regions of positive and negative electrostatic potential within a molecule. Each MEP surface includes a color scale that indicates the extreme values of the electrostatic potential:

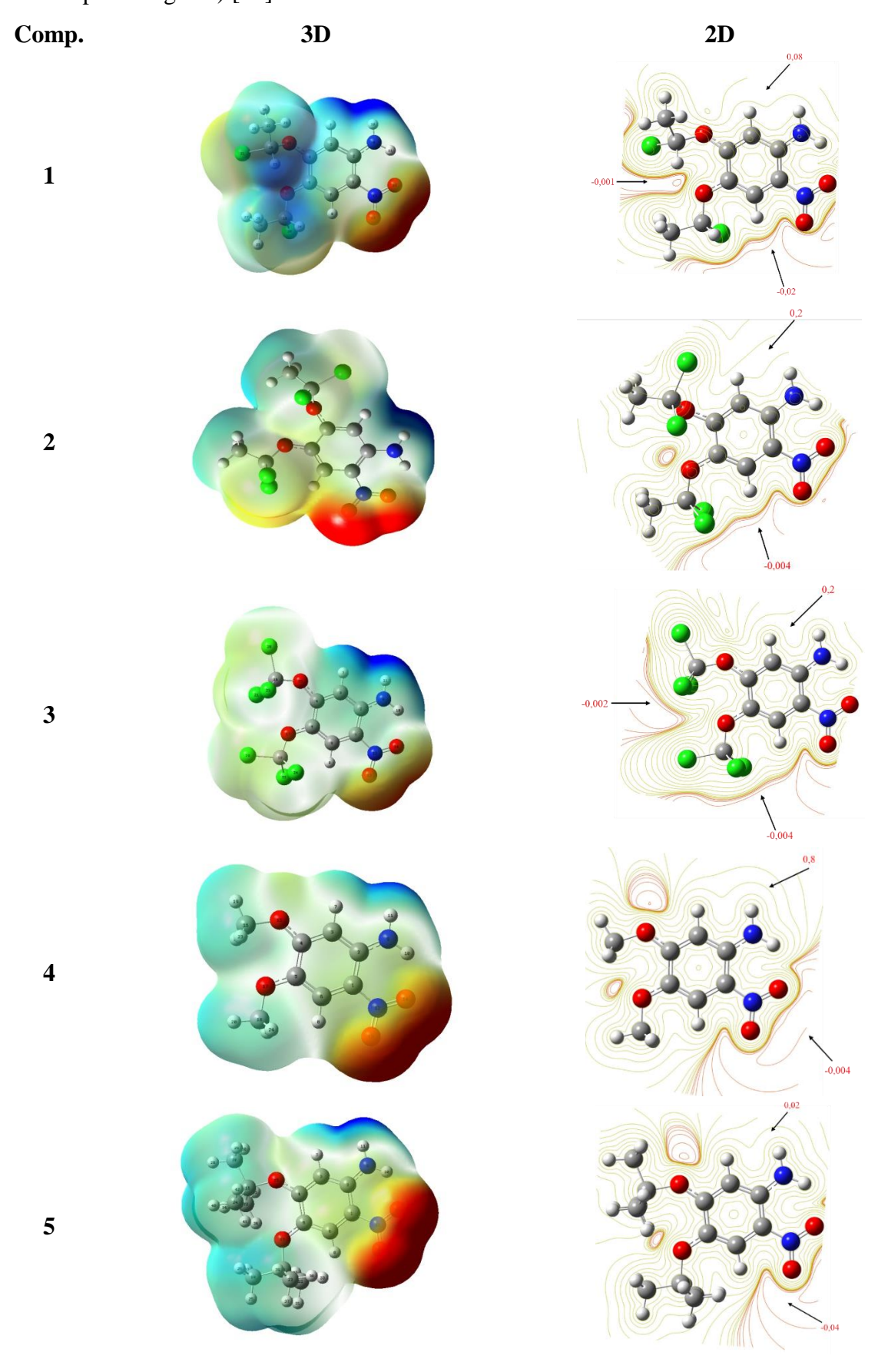
- Red represents the minimum electrostatic potential (regions with excess electrons or loosely bound areas), making these sites prone to electrophilic attack.
- Blue indicates the maximum electrostatic potential (electron-deficient regions), which are more likely to undergo nucleophilic attack [28].

b) 2D-Contours of the Molecular Electrostatic Potential

Building on the previous explanation, if we plot all the MEP surfaces corresponding to different iso-surface values, the standard view shows only the outermost surface. To visualize all MEP surfaces, each contour can be drawn around the molecule.

- Outer contours correspond to lower iso-surface values.
- Inner contours representhigher iso-surface values.

The color interpretation (red highlights potential electrophilic sites, while blue signals nucleophilic regions) [28].



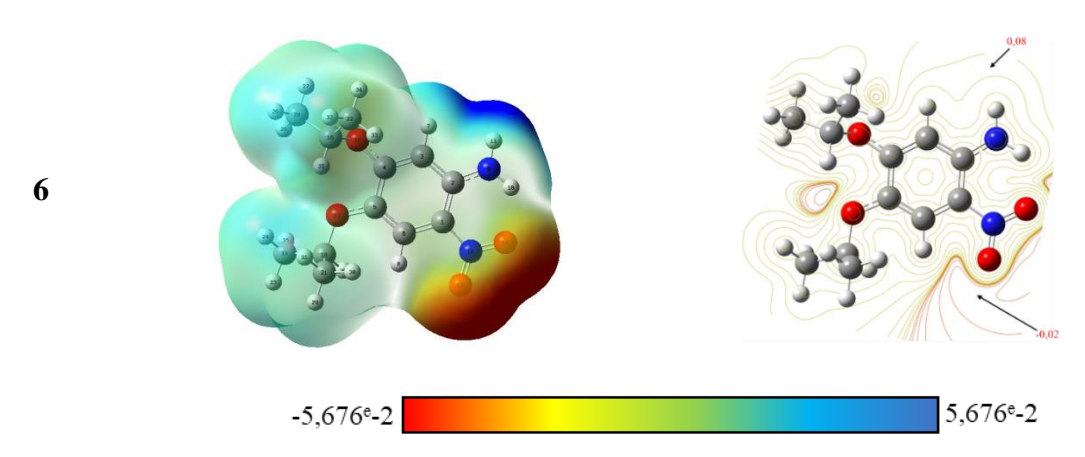


Figure II. 4: 3D-MESP surface map and 2D-MESP contour map for 4,5-dialkoxy-2-nitroanilines

The MESP surface map and contour map of 4,5-dialkoxy-2-nitroanilines (Figure II.4) show that the electronegative potential region (in red) is located around the nitro group, making nucleophilic approach to the C5 atom unfavorable. On the other hand, the electropositive region (in blue) is located around the amine group, near the C4 atom, making nucleophilic approach to this atom possible.

II.6. Conclusion

In this section, a theoretical method based on conceptual-DFT theory was performed to investigate the regioselectivity of the transetherification of 4,5-dialkoxy-2-nitroanilines.

Carbon C4 is the preferred site for nucleophilic attack due to several complementary factors. The inductive effect of the NO₂ group plays a key role: the nitro group, through its electronwithdrawing effect, removes electron density from the benzene ring, making the ortho (C2) and para (C4) carbons more electrophilic. Interaction with the NH₂ group also comes into play: the amine, through its mesomeric donor effect (+M), tends to push electrons towards the ring, but this influence ispartially offset by the NO₂ group,this results in a more pronounced positive partial charge on C4, where the attractive effect of the NO₂ prevails. Furthermore, the stability of the intermediate formed upon nucleophilic attack is enhanced by a stabilizing resonance between the NO₂ and NH₂ groups, which does not occur at the other positions. Finally, steric accessibility favors C4: geometrically less crowded than ortho carbons (C2 and C6), it allows easier approach of the nucleophile, a crucial factor if spatial constraints, for example imposed by an enzymatic active site, come into play.

References

- [1] K. Kaur, S.R. Patel, P. Patil, M. Jain, S.I. Khan, M.R. Jacob, S. Ganesan, B.L. Tekwani, R. Jain, Bioorganic & Medicinal Chemistry .2007,15, 915.
- [2] J. Grolik, P. Reka, M. Gorczyca, K. Stadnicka, Tetrahedron Lett. 2022, 99, 153830.
- [3] S. Kenouche, A. Belkadi, R. Djebaili, N. Melkemi. High regioselectivity in the amination reaction of isoquinolinequinone derivatives using conceptual DFT and NCI analysis. Journal of Molecular Graphics and Modelling Elsevier, 2021 104 (5), 107828-107840.
- [5] Gaussian 09, Frisch MJ, Trucks GW, Schlegel HB, Scuseria GE, Robb MA, Cheeseman JR, Scalmani G, Barone V, Mennucci B, Petersson GA, Nakatsuji H, Caricato M, Li X, Hratchian HP, Izmaylov AF, Bloino J, Zheng G, J. Sonnenberg L, Hada M, Ehara M, Toyota K, Fukuda R, Hasegawa J, Ishida M, Nakajima T, Honda Y, Kitao O, Nakai H, Vreven T, Montgomery JA., Peralta JE, Ogliaro F, Bearpark M, Heyd JJ, Brothers E, Kudin KN, Staroverov VN, Keith T, Kobayashi R, Normand J, Raghavachari K, Rendell A, Burant JC, Iyengar SS, Tomasi J, Cossi M, Rega N, Millam JM, Klene M, Knox JE, Cross JB, Bakken V, Adamo C, Jaramillo J, Gomperts R, Stratmann RE, Yazyev O, Austin AJ, Cammi R, Pomelli C, Ochterski JW, Martin RL, Morokuma K, Zakrzewski VG, Voth GA, Salvador P, Dannenberg JJ, Dapprich S, Daniels AD, Farkas O, Foresman JB, Ortiz JV, Cioslowski J, Fox DJ, Gaussian Inc. Wallingford CT (2010).
- [6] Par RG, Yang W. In Density-functional theory of atoms and molecules; Oxford Univ. Press: Oxford, 1989.
- [7] Becke, AD. J Chem Phys 1993, 98: 1372-77.
- [8] Becke, AD. J Chem Phys 1993, 98: 5648-5652.
- [9] R. Djebaili, N. Melkemi, S. Kenouche, I. Daoud, Mohammed Bouachrine, Halima Hazhazi, Toufik Salah, Combined Conceptual-DFT, Quantitative MEP Analysis, and Molecular Docking Study of Benzodiazepine Analogs, Orbital: Electron. J. Chem. 2021, 13(4), 301-315.
- [10] A. Klamt, G. Schüürmann, COSMO: a new approach to dielectric screeningin solvents with explicit expressions for the screening energy and its gradient, J. Chem. Soc., Perkin Trans. 2. 5,1993,799-805.
- [11] Karabacak M, Sinha L, Prasad O, Asiri AM, Cinar M. J. Spectrochimica. Acta. Part A: Molecular and Biomolecular Spectroscopy .2013;115: 753-66.
- [12] Y. Jincheng, Q.S.Neil, Y.Weitao, Describing Chemical Reactivity with Frontier Molecular Orbitalets, 2022, 2(6).
- [13] R. G. Pearson, J. Am. Chem. Soc. 1983, 85, 3533.
- [14] R. G. Pearson, J. Am. Chem. Soc. 1963, 85, 3533.
- [15] R. G. Pearson, Science, 1966, 151, 172.
- [16] R. G. Pearson, J. Songstad, J. Am. Chem. Soc. 1967, 89, 1827.

- [17] R. G. Pearson, J. Am. Chem. Soc. 1983, 105, 7512
- [18] R G. Parr, L V .Szentpaly, S Liu, J. Am. Chem. Soc. 1999, 121, 1922.
- [19] L. R. Domingo, M.J. Aurell, P. Perez, R. Contreras, Tetrahedron. 2002, 58, 4417.
- [20] L. R. Domingo, M. Duque-Noreña, E. Chamorro, J. Mol. Struct. 2009, 895,86.
- [21] S. Azhagiri, S. Jayakumar, S. Gunasekaran, S. Srinivasan, Spectrochimica Acta Part A: Molecular and Biomolecular Spectroscopy.2014, 124, 199–202
- [22] R. G. Pearson, «Hard and Soft Acids and Bases». Dowden. Hutchinson et Ross:Stroudenbury,PA, 1973.
- [23] P. Geerlings, F. De Proft, W. Langenaeker, Chem. Rev. 2003, 103; 1793.
- [24] R. G. Parr, W. Yang, J. Am. Chem. Soc. 1984, 106, 4049.
- [25] W. Yang, W. J. Mortier, J. Am. Chem. Soc. 1986, 108, 5708.
- [26] P. K. Chattaraj, S. Nath, A. B. Sannigrahi, J. Phys. Chem. 1994, 98, 9143
- [27] C.H. Suresh & G.S. Remya, Molecular electrostatic potential analysis: A powerful tool tointerpret and predict chemical reactivity, Computational Molecular, 2,2022.
- [28] K. Choudhary, K.F. Garrity, F. Tavazza, Data-driven discovery of 3D and 2D thermoelectric, Condensed Matter, 2020.

Chapter III:

In silico study of the antidiabetic properties of 5-(4-methylpiperazin-1-yl)-2-nitroaniline and its analogs.

III.1. Introduction

Molecular docking is an essential approach in medicinal chemistry and rational drug design that allows the modeling of the interactions between a bioactive molecule (ligand) and its biological target, usually an enzyme or receptor [1]. This technique is based on the prediction of the optimal conformation of the ligand within the active site of the protein and the estimation of the binding affinity by energy scores. It plays a crucial role in the virtual screening of chemical compounds to identify those with high therapeutic potential before any experimental validation. In this context, the study by Sun et al. [2] is part of an effort to discover new natural inhibitors of dipeptidyl peptidase-4 (DPP-4), a key enzyme involved in blood glucose regulation and a target for the treatment of type 2 diabetes. Combining a pharmacophoric model derived from known inhibitors with molecular docking simulations, the authors screened a library of compounds from Chinese medicinal plants. This screening resulted in the selection of 45 candidates, among which two compounds showed remarkable binding affinity and stable interactions with DPP-4 functional residues. These results suggest that certain natural molecules have interesting potential as structural bases for the development of new anti-diabetic agents targeting DPP-4.

III.2. Brief overview of in silico methods in drug discovery

III.2.1. Molecular docking

Molecular docking is a powerful and essential computational method in the fields of pharmaceutical development, structural biology and the study of biomolecular interactions. It involves predicting how a small molecule, often a drug candidate, interacts with a target biomolecule such as a protein or DNA, by assessing the spatial and energetic compatibility between the ligand and the active site of the receptor. This technique not only allows the identification of new bioactive compounds, but also the optimization of existing ones, while providing a better understanding of the mechanisms of interaction between molecules. This technique not only allows the identification of new bioactive compounds, but also the optimization of existing ones, while providing a better understanding of the mechanisms of interaction between molecules. Docking relies on algorithms that generate and rank different ligand-receptor conformations according to their binding energy, with an accurate scoring function being crucial to discriminate high-affinity ligands from low-affinity ones. It finds

major applications in structure-based drug design, virtual screening of chemical libraries and lead optimization. In the case of structural design, the three-dimensional structure of the target guides the selection of ligands capable of efficiently interacting with the active site. Virtual screening accelerates the identification of potential candidates, while lead optimization relies on successive docking iterations aimed at improving affinity and pharmacological properties. This constantly evolving field has been enriched with numerous methodologies to address the specific challenges of drug design and molecular interaction analysis. This report provides an in-depth analysis of the principles, methods, and applications of docking, highlighting their central role in understanding and exploiting molecular interactions in therapeutic contexts [3].

III.2.2. Types of molecular docking

Molecular docking studies can be of three types, namely rigid docking, flexible-rigid docking, and flexible docking (based on the flexibility of the interacting molecules, receptor, and ligand), as shown in figure III.1 [4]. Flexible docking provides more reliable and accurate results because the relative bond angle and bond length of the molecules can vary. Pagadala and co-workers have presented a review of different molecular docking programs based on rigid and flexible docking [5].

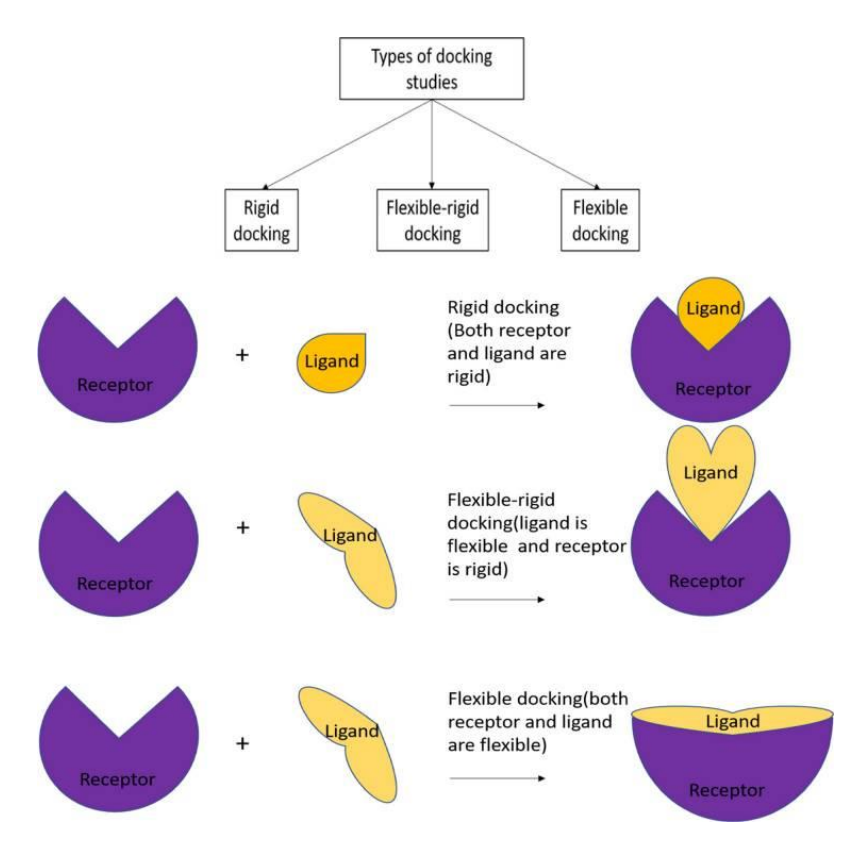


Figure III. 1: Different types of molecular docking studies based on flexibility of receptors/ligands considered in molecular interaction

Rigid docking: In rigid docking, both ligand and receptor molecules are considered rigid bodies. Their shape is not changed and thus the internal geometry of each molecule is kept fixed. Their position can be varied, so only the translational and rotational degrees of freedom are considered. This is an early docking method that can be performed between macromolecules, such as two protein molecules, and the result is less accurate and unreliable and is therefore less commonly used in current docking studies. The lock-and-key principle can be used in this method [6].

<u>Flexible-rigid</u>: This is a semi-flexible docking method. In this case, either the ligand or the receptor is considered as a rigid body. Usually, the shape of the receptor is kept fixed and the conformation of the ligand is varied. This method gives more accurate and reliable results than the rigid docking method and is therefore often used.

Flexible (soft) docking: This is a fully flexible docking method in which both the ligand and the receptor are considered as flexible bodies, i.e., a series of rotations of the molecules (both receptor and ligand) is performed to search for the optimized conformation and orientation of the molecules to interact with each other. The shape of the molecule can be varied by changing the torsion angles and rotatable bonds. This method results in prediction of the docked conformation with high accuracy, which is most likely to resemble the experimental results, but may require extensive computation and time [6].

III.2.3. Molecular docking procedure

a. Ligand preparation

Generation or import of 3D structures (ChemDraw, Avogadro, PubChem...), geometric optimization by force field and selection of a set of low-energy conformers to cover molecular flexibility [7].

b. Target preparation

Obtain 3D structure (PDB), clean up (water/ion removal), assign tautomeric states and protonation at physiological pH, then local minimization to remove steric constraints [8].

c. Active site recognition

Definition of a docking box around the co-crystallized ligand or prediction of cavities (blind docking or pocket tools) if the site is unknown [9].

d. Docking

Execution with software (AutoDock Vina, Glide...), flexible parameterization (ligand and/or receptor), computational grid and generation of multiple poses per ligand [10].

e. Validation and evaluation

RMSD calculation (< 2 Å) to validate reproduction of experimental binding mode [11]. Ranking by binding free energy (Δ Gbind) and accurate re-scoring (MM-GBSA/MM-PBSA) to refine selection. Analysis of key interactions (H-bonds, hydrophobes, π - π) to retain the best candidates [12].

III.2.4. Molecular Dynamics (MD) simulations

Is a numerical simulation method based on Newton's laws of classical mechanics that models the motion and interactions of atoms or molecules over time. Each particle in the system is subject to forces derived from a molecular force field, and its equations of motion are integrated step by step to generate an atomic trajectory. This approach provides a Dynamics view of conformational changes - for example, in proteins during ligand binding - and sheds light on functional mechanisms that are often inaccessible using experimental methods alone [13-15].

Molecular Dynamicss simulations are divided into three main phases: (1) initialization, during which the initial atomic configuration (initial positions and velocities derived from a Maxwell-Boltzmann distribution at the target temperature) is constructed from experimental or modeled structures; (2) thermalization, during which a thermostat adjusts kinetic and potential energies until the temperature stabilizes around the set point (e.g., 300 K); and (3) production, after a period of equilibration (ps-ns), during which trajectories are recorded under controlled temperature (and pressure) conditions.300 K); and (3) production, after a period of equilibration (ps-ns), during which trajectories are recorded under controlled temperature (and pressure) conditions. Post-simulation analysis includes Root-Mean-Square Deviation (RMSD) calculation to quantify structural stability and energy profile evaluation to characterize the balance between potential and kinetic energy [16].

III.2.5. Bioisosteric Conversion

Bioisosteric substitution transforms an active compound into another compound by exchanging one atom or group of atoms with another group of atoms with another group of structurally similar atoms [17]. The resulting new compound retains its biological activity while attempting to improve the undesirable properties of the original compound. We have found numerous software packages, and in our case, we used the Molopt online web server [18].

III.3. Molecular docking/Dynamics simulations of 5-(4-methylpiperazin-1-yl)-2-nitroaniline and its analogs as SIRT6 inhibitors

III.3.1. Materials and methods

III.3.1.1. Ligands preparation

In this study we have selected a series of 5-(4-methylpiperazin-1-yl)-2-nitroaniline and its analogs. The compound 5-(4-methylpiperazin-1-yl)-2-nitroaniline (figure III.2) has been synthesized and evaluated for its high antidiabetic activity [2].

Figure III. 2: Structure of 5-(4-methylpiperazin-1-yl)-2-nitroaniline.

The 3D structures of the 5-(4-methylpiperazin-1-yl)-2-nitroaniline analogs (figure III.2) were obtained using the fast online tool MolOpt [18] (https://xundrug.cn/molopt/silicoopt), which plays a key role in the ligand preparation phase of molecular modelling. It ensures that the 3D structure submitted for docking or simulation is chemically correct and energetically plausible, thus improving the reliability of the results obtained. All structures were optimized using the semi-empirical AM1 method implemented in the Hyperchem 8.0.8 software

(version 8.0.8, Hypercube, USA, http://www.hyper.com). In addition, all these structures were converted to extension. *mdb for use as MOEdocking input.

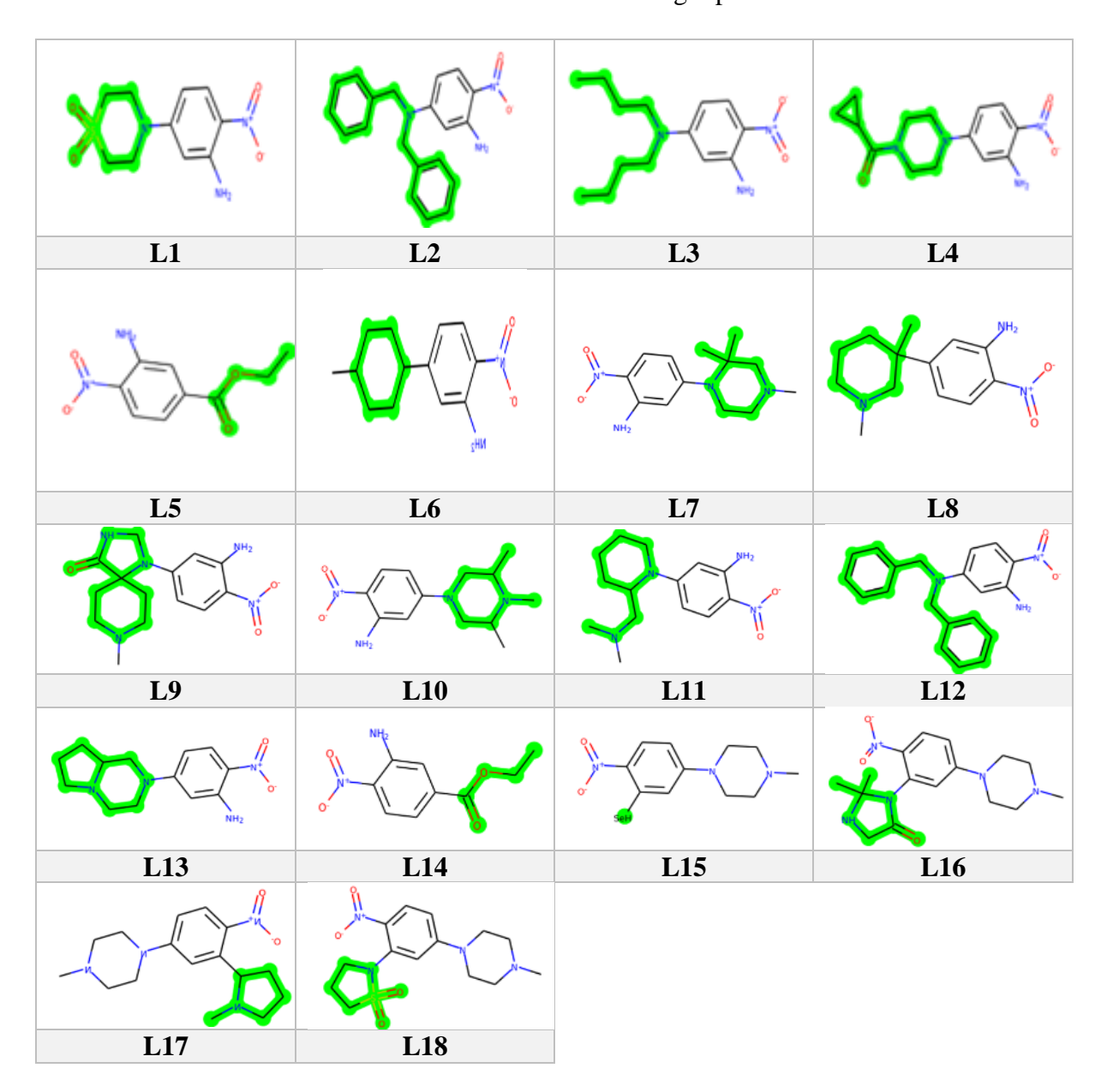


Figure III. 3: Structures of the 5-(4-methylpiperazin-1-yl)-2-nitroaniline analogs.

III.3.1.2. Target preparation

SIRT6 is a key enzyme in carbohydrate metabolism whose inhibition promotes the expression of transporters such as GLUT1, thereby improving glycemic regulation. This property positions SIRT6 as a promising anti-diabetic target [2,19]. Its crystal structure, available under PDB: 3K35, provides a reference model for the design of inhibitors using molecular modeling approaches.

The 3D structure of this target (Figure III.4) was obtained from the Protein Data Bank (www.rcsb.org/pdb) and selected as the anti-diabetic target. The cellular protein SIRT6 (PDB ID: 3K35) complexed with the ligand ADENOSINE-5-DIPHOSPHORIBOSE (APR) (Table III.1) [20].

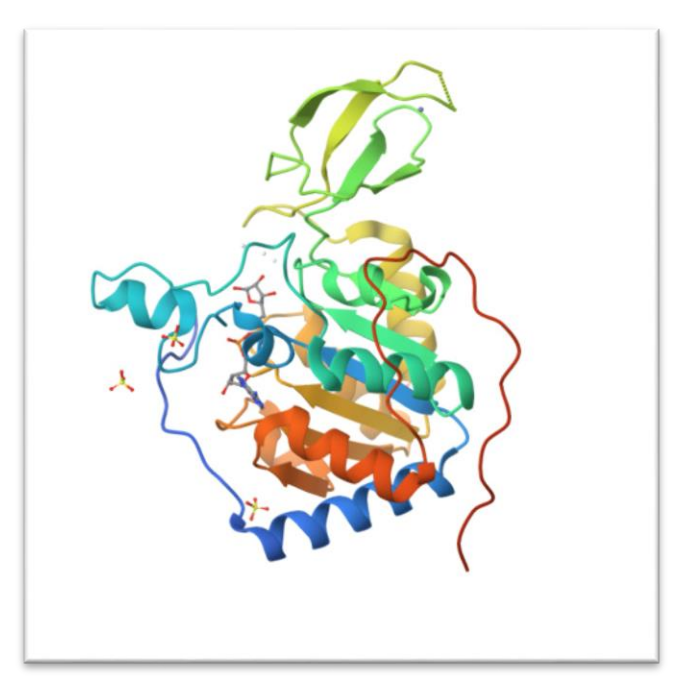


Figure III. 4: 3D structure of the 3K35 receptor.

Table III. 1- Some characteristics of the targets selected for the study.

Target	Co-crystallized ligand	Classification	Total Structure Weight	Chains	Resolution
PDB ID: (3K35)	NH ₂ N N N N N N N N N N N N N N N N N N N	HYDROLASE	215.88 KDa	A	2.00 Å

III.3.1.3. Molecular docking protocol

Molecular docking calculations were performed using MOE software to find the best ligand placement in the target's active site, which allows for the establishment of different types of interactions between these entities [21].

Active site residues of target

The "Site Finder" option [21], integrated in the MOE2015 software, allowed us to identify and explore the active sites of the selected enzyme in this study (figure III.5). The following Table III.2 show all residues that form this site.

PDB	Size ^(a)	PLB ^(b)	Hyd ^(c)	Side ^(d)	Residues
3K35	324	3.49	73	138	LYS13, GLU20, GLY50, ALA51, GLY52, ILE53, SER54, THR55, ALA56, GLY58, ILE59, PRO60, ASP61, PHE62, ARG63, GLY64, PRO65, HIS66, GLY67, VAL68, TRP69, PRO78, LYS79, PHE80, ASP81, PHE84, GLN111, ASN112, VAL113, ASP114, HIS131, MET134, MET155, GLY156, ILE183, LEU184, ASP185, TRP186, GLU187, ASP188, SER189, GLY212, THR213, SER214, LEU215, GLN216, ILE217, ARG218, SER220, GLY221, VAL237, ASN238, LEU239, GLN240, GLY254, TYR255, VAL256, ASP257

Table III. 2: Information of the selected target (3K35).

(a): Number of alpha spheres comprising the site, (b): Propensity score for the ligand for the contact residues in the receptor, (c): The number of hydrophobic contact atoms in the receptor, (d): The number of side-chain contact atoms in the receptor.

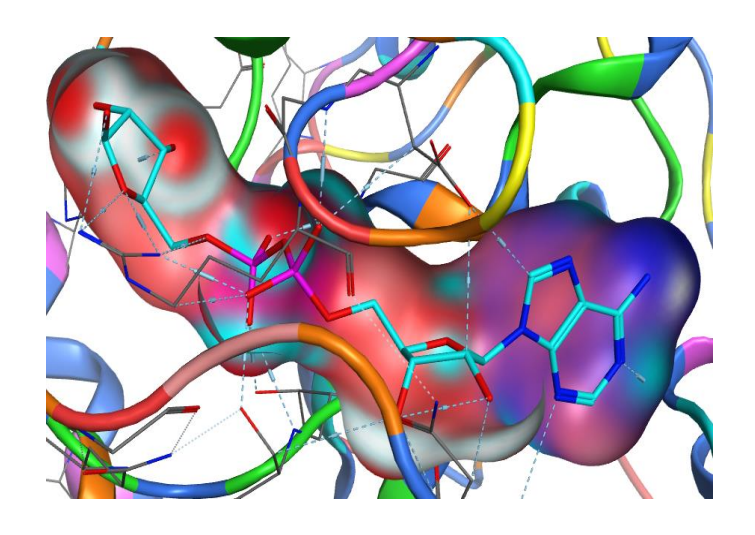


Figure III. 5: Active site of the selected target.

Method validation

In addition, the method was validated by redocking co-crystallized ligand (APR) to their target, and we found that the obtained RMSD values obtained were less than 2 Å (Table III.3), indicating that the docking method (software) used is accurate and reliable. (software) is accurate and reliable (figure III.6).

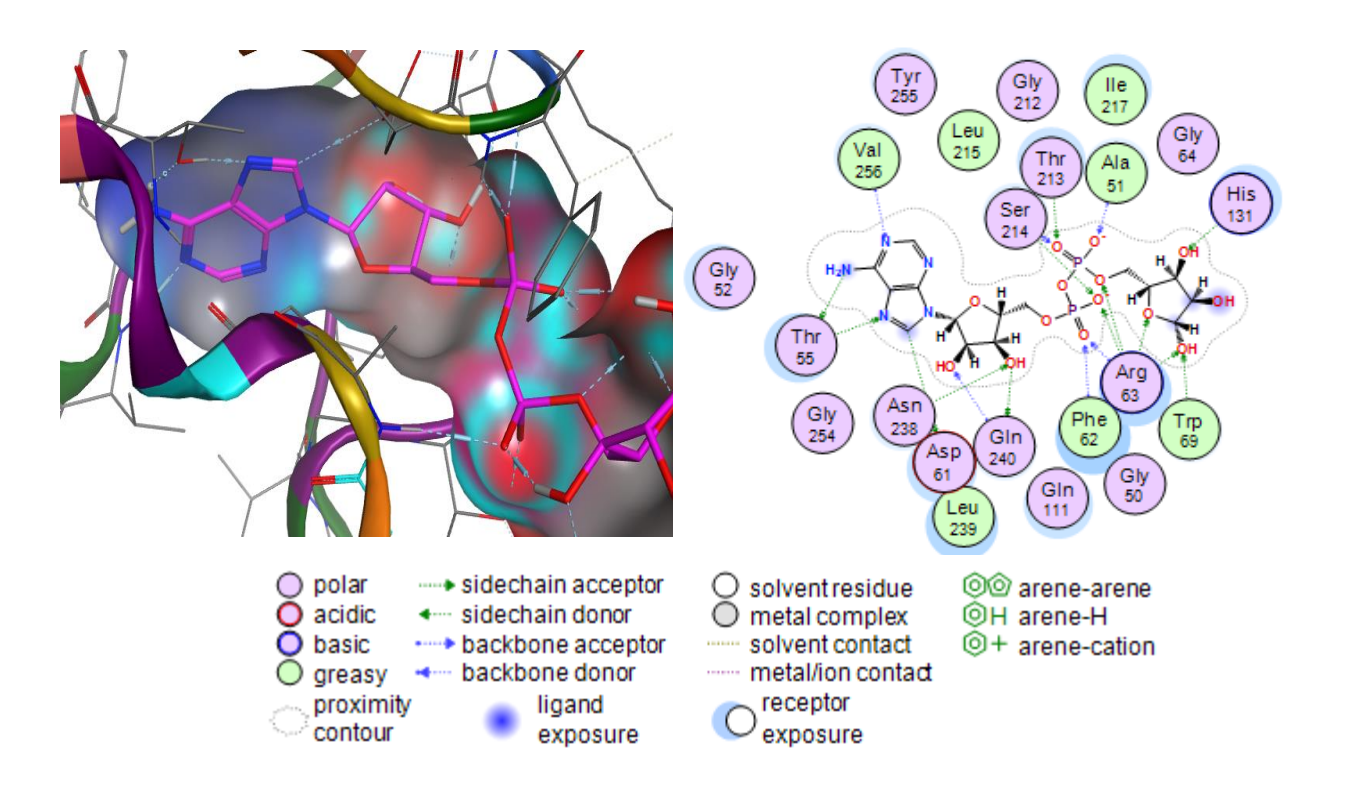


Figure III. 6: 3D crystal structure of 3K35 complexed with APR (co-crystallized ligand) and 2D representation of the interactions of APR with the binding pocket of 3K35 receptor.

III.3.1.3. Molecular Dynamics simulation

To further validate the docking conformer interactions, top-rated complexes for this target were selected for molecular Dynamics simulation. MOE software was used to perform molecular Dynamics simulation and explore the stability of the six complexes formed by the following ligands: L1, L4, L13, L17, L18 and the synthesized compound (5-(4-methylpiperazin-1-yl)-2-nitrobenzenamine). The MD simulation was performed using the Nose-Poincare-Andersen (NPA) algorithm, which reveals the interactions of amino acid residues in each system [22,23]. The energy minimization step implements the Merck

MMFF94x molecular force field [24]. In addition, a cut-off radius of 8.0 Å was considered for short-range Van der Waals interactions, and the Berendsen thermostat algorithm was used to control the simulation temperature [25]. Next, 100 ps was chosen for the equilibrium time interval, and the production phase was set to 900 ps for each system. All other parameters were left as default. To analyze the conformational stability of the complexes, the fluctuation of the potential energies U (Kcal/mol) was plotted against the simulation time (ps) using Origin pro 2021 6.0 software [26].

III.3.1.4. ADME prediction and physicochemical properties

To study the pharmacoDynamics and pharmacokinetic properties of the selected compounds, various parameters were calculated using the server: SwissADME (http://www.swissadme.ch/) [27].

III.3.2. Results and discussion

III.3.2.1. Molecular docking analysis

After identifying the ideal cavity for the selected target, we performed a molecular docking calculation between the synthesized compound 5-(4-methylpiperazin-1-yl)-2-nitroaniline and 18 analogs (L1-18) with the enzyme active site residues (PDB: 3K35). The results obtained are grouped in Table III.3.

In addition, the interactions of the best positions for each complex were analyzed and visualized using MOE software.

The docking results were analyzed and discussed based on various parameters such as affinity (S-score), RMSD, and interactions (types and distances). Firstly, the stability of the target-compound complex depends on the high affinity between these two entities, which is justified by the negative energy score of the complex formed. Secondly, non-covalent bonds (hydrogen bonds and hydrophobic interactions. . .) ensure the formation of the (target-compound) complex, and they can be classified in the following areas. According to the literature:

- Hydrogen bonding distances between 2.5 and 3.1 Å are considered strong interactions and those between 3.1 and 3.55 Å are considered weak interactions [28].
- Regarding hydrophobic interactions, Janiak [29] suggests that the optimal range for hydrophobic interactions is between 3.3 and 3.8 Å. However, other researchers have suggested a relatively higher range [30,31].

Table III. 3: Docking score energy, RMSD, and interactions between 2-niroaniline compounds and co-crystallized ligand (APR) with residues of the active site residues of the 3K35 target.

			Bonding between atoms and active site residues							
Comp.	S SCORE (Kcal/mol)	RMSD (Å)	Atom of compound	Atom of receptor	Evolved receptor residue	Type of interaction bond	Distance (Å)			
Synthesized compound	-6,449	1,389	O32	N	VAL 256	H-acceptor	3.14			
L1	6.070	1 771	N 12	OE1	GLN 111	H-donor	3.41			
1.1	-6,978	1,771	O 31	ND2	ASN 238	H-acceptor	2.89			
			N 11	О	GLY 212	H-donor	2.83			
			O 14	NHI	ARG 63	H-acceptor	3.52			
L2	-6,476	1,080	O 14	OG	SER 214	H-acceptor	2.72			
			O15	N	PHE 62	H-acceptor	2.94			
			O 15	N	ARG 63	H-acceptor	2.91			
L3		2 (20	O 14	N	GLN 40	H-acceptor	3.16			
L3	-5,993	2,630	6-ring	CDI	LEU 239	pi-H	3.66			
L4	5 04 5	5 01 5	7.017	7.017	0.545	O 33	NHI	ARG 63	H-acceptor	3.36
L/ 1	-7,817	0,545	O 33	OG	SER 214	H-acceptor	2.90			
			N 11	О	GLY 212	H-donor	2.86			
			O 14	NHI	ARG 63	H-acceptor	3.24			
			O 14	OG	SER 214	H-acceptor	2.77			
L5	-6,638	1,285	O15	N	PHE 62	H-acceptor	2.86			
			O15	N	ARG 63	H-acceptor	2.98			
			O17	N	LEU 239	H-acceptor	3.03			
			O17	N	GLN 240	H-acceptor	3.37			
L6	-6,580	1,195	O14	N	VAL 256	H-acceptor	3.23			
L7	-5,771	1,661	O14	N	VAL 256	H-acceptor	2.99			
			N26	OE2	GLU 20	H-donor	2.86			
L8	-5,491	0,655	O14	N	SER 214	H-acceptor	2.98			
			O15	NHI	ARG 63	H-acceptor	3.14			
10	.	0.5	N11	OG	SER 214	H-acceptor	2.91			
L9	-5,456	0,735	O15	N	SER 214	H-acceptor	3.39			
I 10			N11	О	GLY 212	H-donor	2.75			
L10	-6,245	1,754	O14	OG	SER 214	H-acceptor	2.79			

		ı	T	ı	T	,	
			O15	N	PHE 62	H-acceptor	3.00
				N	ARG 63	H-acceptor	2.91
L11	C 295	1.264	N11	О	GLY 212	H-donor	2.98
LII	-6,385	1,364	O15	N	ARG 63	H-acceptor	3.15
			N11	О	GLY 52	H-donor	3.07
L12	-6,515	1,415	O14	N	GLN 240	H-acceptor	3.51
			6-ring	N	ASP 61	Pi-H	4.58
I 12		4.700	N16	N	SER 214	H-acceptor	3.19
L13	-7,290	1,583	6-ring	OG1	THR 213	pi-H	4.07
			N11	О	GLY 212	H-donor	2.87
			O14	NHI	ARG 63	H-acceptor	3.21
			O14	OG	SER 214	H-acceptor	2.75
L14	-6,637	0,863	O15	N	PHE 62	H-acceptor	2.88
			O15	N	ARG 63	H-acceptor	2.95
			O18	N	LEU 239	H-acceptor	3.06
			O18	N	GLN 240	H-acceptor	3.48
			SE33	OE2	GLU 20	H-donor	2.97
L15	-5,787	1,231	SE33	OD1	ASP 61	H-donor	3.29
			N20	N	SER 214	H-acceptor	3.42
L16	7 0.66	1.000	C31	О	GLY 52	H-donor	3.34
L10	-5,866	1,000	O12	N	VAL 256	H-acceptor	2.98
L17	-7,082	1,288	O10	N	LEU 239	H-acceptor	3.00
I 10			O11	N	LEU 239	H-acceptor	2.96
L18	-7,486	1,343	O42	N	GLN 240	H-acceptor	2.82
			N68	OG1	THR 55	H-donor	3.04
			C812	OD1	ASP 61	H-donor	3.24
			O3'23	OE1	GLN 240	H-donor	2.66
			N111	N	VAL 256	H-acceptor	3.01
			N711	OG1	THR 55	H-acceptor	2.77
APR	-11,594	1,857	O2'19	N	GLN 240	H-acceptor	2.89
			O3'23	ND2	ASN 238	H-acceptor	2.96
			O1A33	N	PHE 62	H-acceptor	2.86
			O1A33	N	ARG 63	H-acceptor	2.78
			O2A34	NH1	ARG 63	H-acceptor	2.73
			O2A34	OG	SER 214	H-acceptor	2.60

	OB137	OG1	THR 213	H-acceptor	2.54
	OB137	N	SER 214	H-acceptor	3.22
	O2B38	N	ALA 51	H-acceptor	3.28
	O5D39	NH1	ARG 63	H-acceptor	2.76
	O4D43	NH1	ARG 63	H-acceptor	2.98
	O4D43	NH2	ARG 63	H-acceptor	2.96
	O1D44	NH2	ARG 63	H-acceptor	3.09
	O1D44	NE1	TRP 69	H-acceptor	2.97
	O3D52	ND1	HIS 131	H-acceptor	3.19
	O2A34	NH1	ARG 63	Ionic	2.73

Molecular docking results for the antidiabetic synthesized compound (5-(4-methylpiperazin-1-yl)-2-nitroaniline) and its analogs (L1-L18) with the SIRT6 target (crystal structure 3K35) show different interaction profiles and different binding affinities. Table III.3 summarizes the binding energies, RMSD values and interaction types observed between these ligands and SIRT6 active site residues.

The synthesized compound has score energy of -6.45 kcal/mol and RMSD of 1.39 Å. It forms a single hydrogen bond (H-receptor) with residue VAL 256 via the O32 atom of the ligand and the N atom of the receptor, with a distance of 3.14 Å. This moderate interaction suggests that a modification of the basic structure could improve the stability and affinity of the complex.

The analog L4 stands out as the best candidate, with score energy of -7.82 kcal/mol and a very low RMSD of 0.55 Å, suggesting a very stable and well anchored position. It forms several hydrogen bonds with ARG63 (3.36Å) and SER 214 (2.90 Å), key residues in the active site.

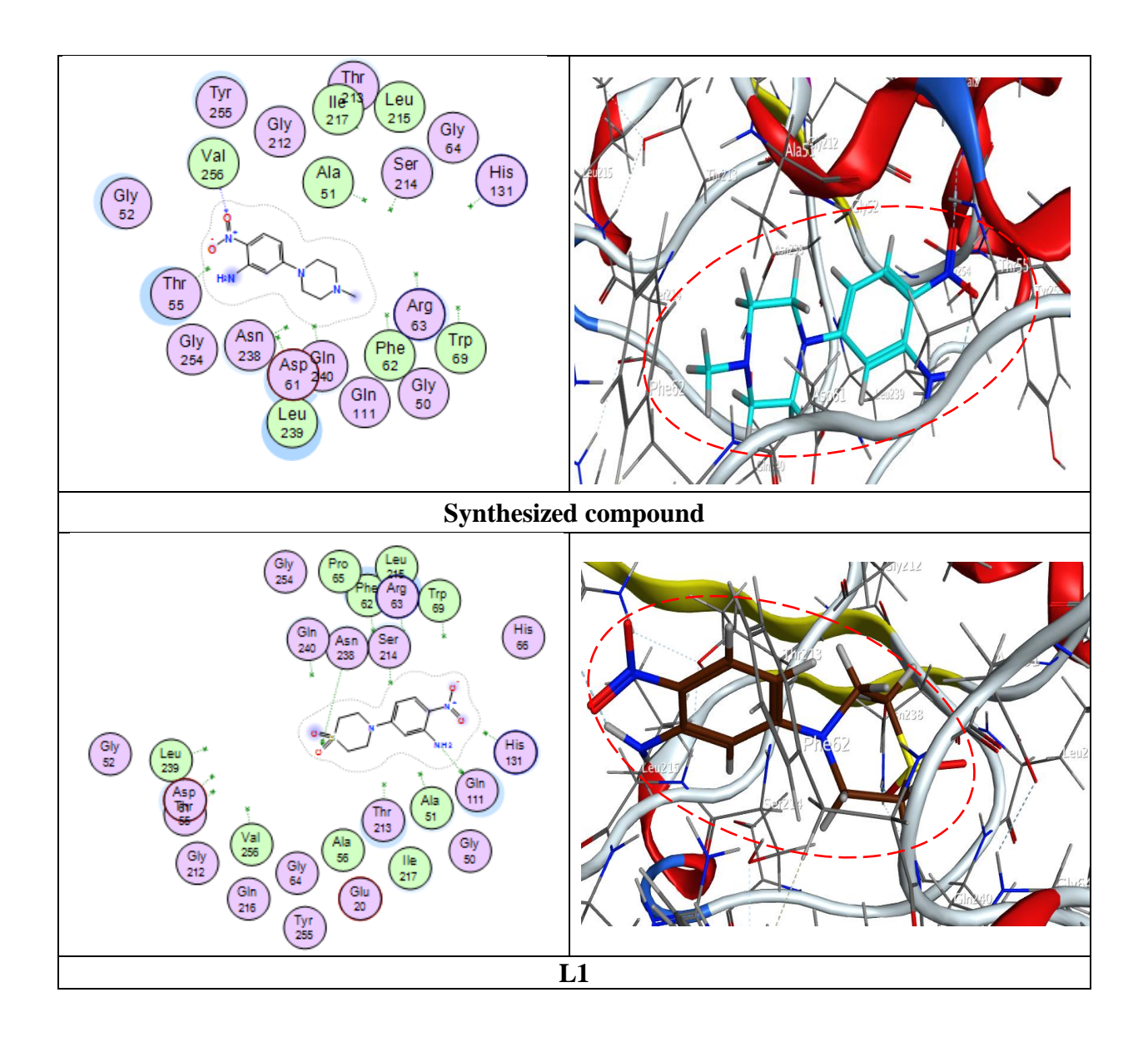
The analog L18 also shows good binding affinity, with a score of -7.49 kcal/mol. In particular, it interacts with LEU 239 and GLN 240, the latter forms strong hydrogen bonds (2.96 and 2.82, respectively), which considerably increases the stability of the complex.

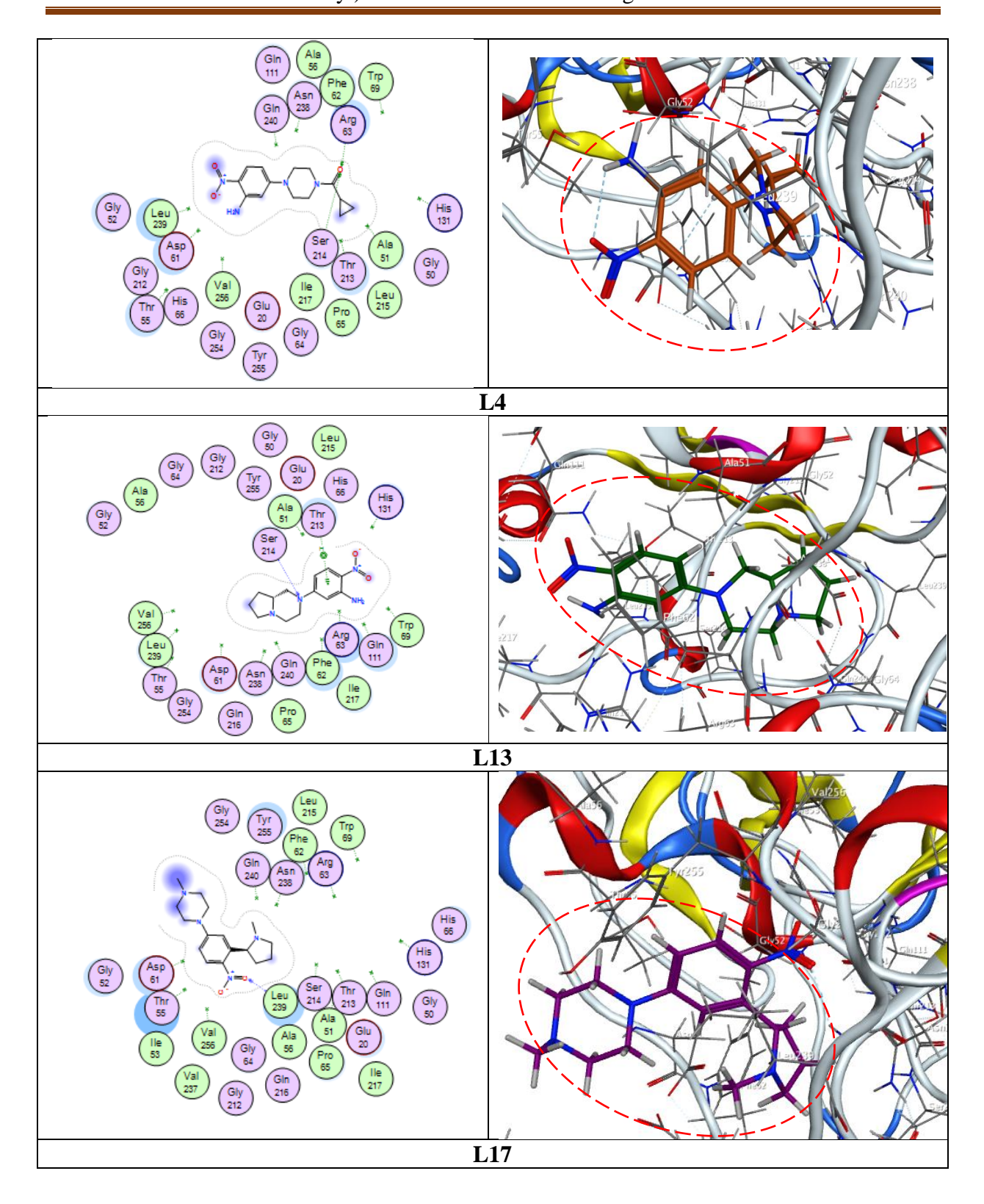
The compound L13, has a score energy of -7.29 kcal/mol, forms a hydrogen bond with SER 214 (3.19 Å), as well as a hydrophobic (pi-H) interaction with THR 213 (4.07 Å), reflecting a balanced bond between polar and non-polar interactions.

The compound L17 shows a score energy of -7.08 kcal/mol. It interacts with LEU 239 (H-acceptor; 3.00 Å). Finally, L1, with score energy of -6.98 kcal/mol, forms H-donor hydrogen bonds with GLN 111(3.41Å) and H-acceptor hydrogen bonds with ASN 238 (2.89Å).

Overall, derivatives L4 and L18 stand out for their low binding energies and the quality of their interactions with the active pocket of 3K35. These results suggest their potential as inhibitors of SIRT6, a target involved in several metabolic pathways associated with diabetes diseases.

These results are illustrated in Figure III.7, which shows in 2D and 3D the interactions formed between the synthesized compound and the best analogs (L1, L4, L13, L17 and L18) with the active site residues of the SIRT6 receptor (3K35).





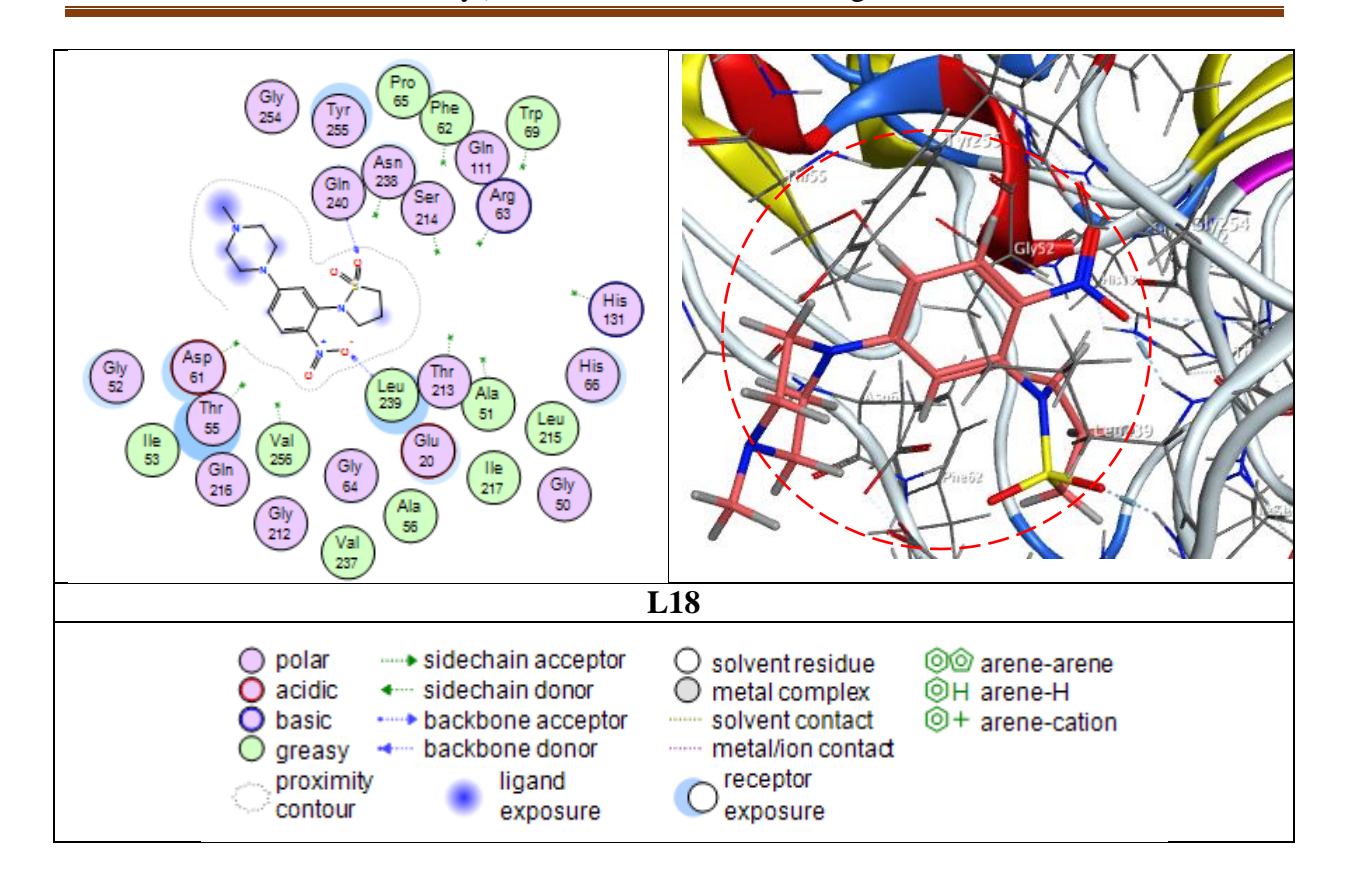


Figure III. 7: 2D and 3D interactions formed between the synthesized compound and the best analogs (L1, L4, L13, L17 and L18) with the active site residues of the SIRT6 receptor (3K35).

III.3.2.2. Molecular Dynamics analysis

The best complexes obtained by molecular docking calculations were validated by molecular Dynamics simulations. The simulation was carried out for 1000 ps (100 ps equilibrium and 900 ps production) to verify the stability of these complexes.

Figure III.8 shows the variation of the potential energy of the complexes (3K35-synthesized compound, 3K35-L1, 3K35-L4, 3K35-L13, 3K35-L17 and 3K35-L18) as a function of time during the molecular Dynamics's simulations.

We observe that for all complexes significant fluctuations in the potential energy appear during the first 100 picoseconds (ps), which is typical for the initial relaxation phase of the system after energy minimization. This phase reflects the adaptation of the ligand to the active site of the protein.

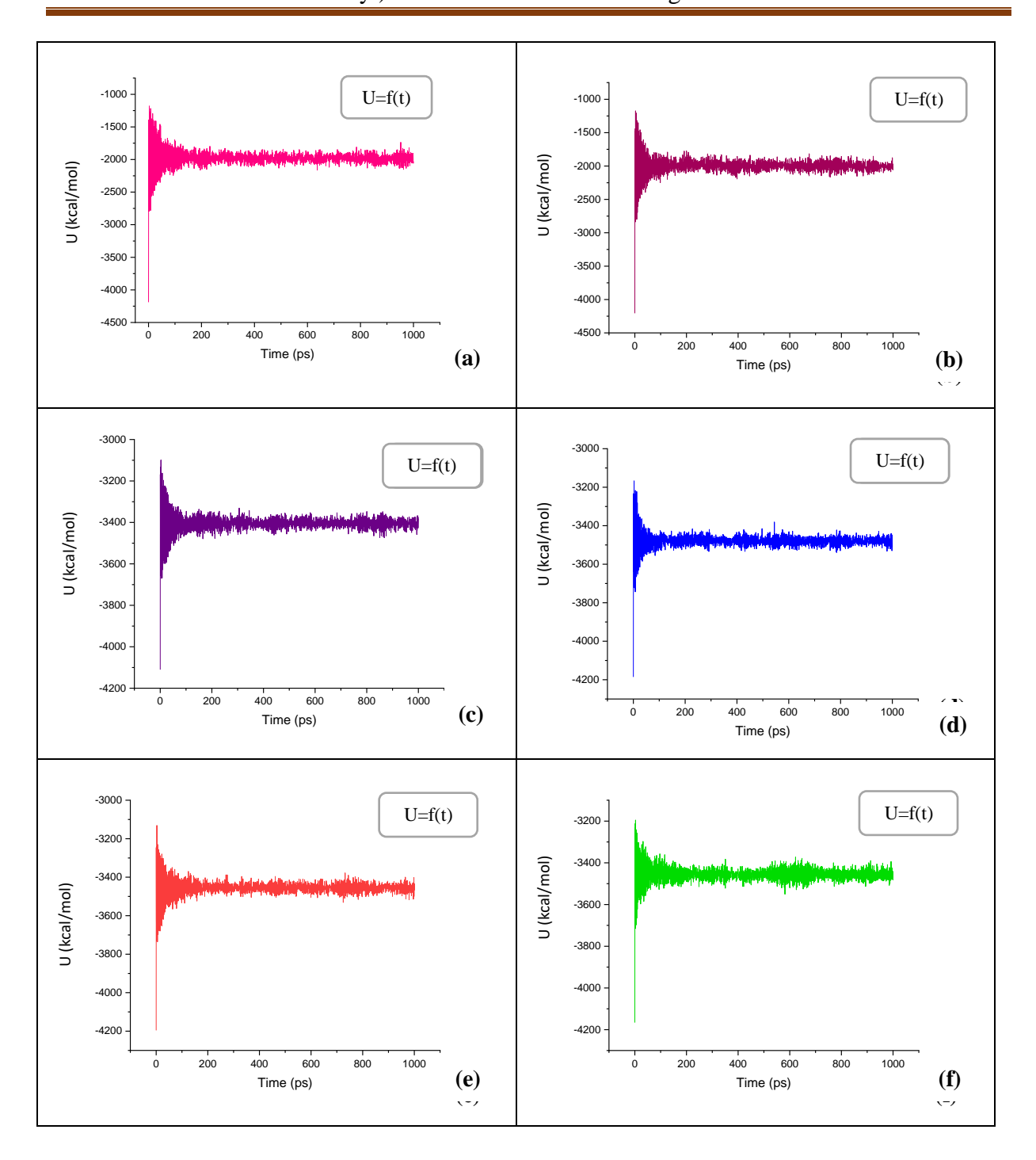


Figure III. 8 : Potential energy plot of the synthesized compound and the top-scoring five hits with 3K35 as a function of simulation time.

(a): synthesized compound, (b): L1, (c): L4, (d): L13, (e): L17, and (f): L18.

Subsequently, between 100 ps and about 600 ps, there is a tendency for the potential energy of all the complexes studied to stabilize progressively. Complexes 3K35-L4, 3K35-L13, 3K35-L17 and 3K35-L18 show a relatively smooth and stable energy curve from this

intermediate phase, reflecting good structural integration and stable interaction of these compounds with the 3K35 target (Figure III. 8).

In contrast, the 3K35-synthesized compound and 3K35-L1 complexes show more pronounced fluctuations beyond 100 ps, reflecting less energy stability during the equilibration phase. The complex 3K35-L13 (Figure III.8 d) also shows fluctuations, although they are less pronounced. The complex K35-L17 (Figure III.7e) reaches a slightly later stability, but remains relatively consistent with the other derivatives.

Finally, over the 600-1000 ps period, all complexes converge to a nearly constant potential energy, confirming that the systems have reached a stable state by the end of the simulation. This stabilization is an essential validity criterion in molecular Dynamics studies, indicating that the ligand-receptor interactions are maintained over time without major perturbations.

III.3.2.3. Protein-ligand interactions after MD simulations

The MD simulation results (the binding interactions) are summarized in Table III.4.

Table III.4 shows that the results obtained from MD simulations are significantly different from those obtained by molecular docking simulation.

Table III. 4: Results of a molecular Dynamics study of the best score of the six ligands in the active site of 3K35

	Bonding between atoms and active site residues										
Comp.	Atom of compound	Atom of receptor residue		Type of interaction bond	Distance (Å)						
	N17	NH2	ARG 246	H-acceptor	3.33						
Synthesized	O32	NZ	LYS 243	H-acceptor	3.34						
compound	O33	NH1	ARG 218	H-acceptor	2.98						
	O33	NH2	ARG 218	H-acceptor	2.95						
	N12	0	GLU 187	H-donor	3.03						
L1	O30	CE	LYS 13	H-acceptor	3.10						
	O31	N	ARG 218	H-acceptor	3.35						
	N11	N	GLY 14	H-acceptor	2.88						
L4	O14	NZ	LYS 13	H-acceptor	3.24						
	O15	NZ	LYS 13	H-acceptor	3.05						
T 10	N16	NE	ARG 74	H-acceptor	3.29						
L13	N22	NH2	ARG 74	H-acceptor	3.15						
L17	O10	NH2	ARG 7	H-acceptor	2.84						
	C38	OE1	GLU 73	H-donor	3.17						
L18	O10	NH2	ARG 74	H-acceptor	2.67						
	O42	NH2	ARG 74	H-acceptor	2.71						

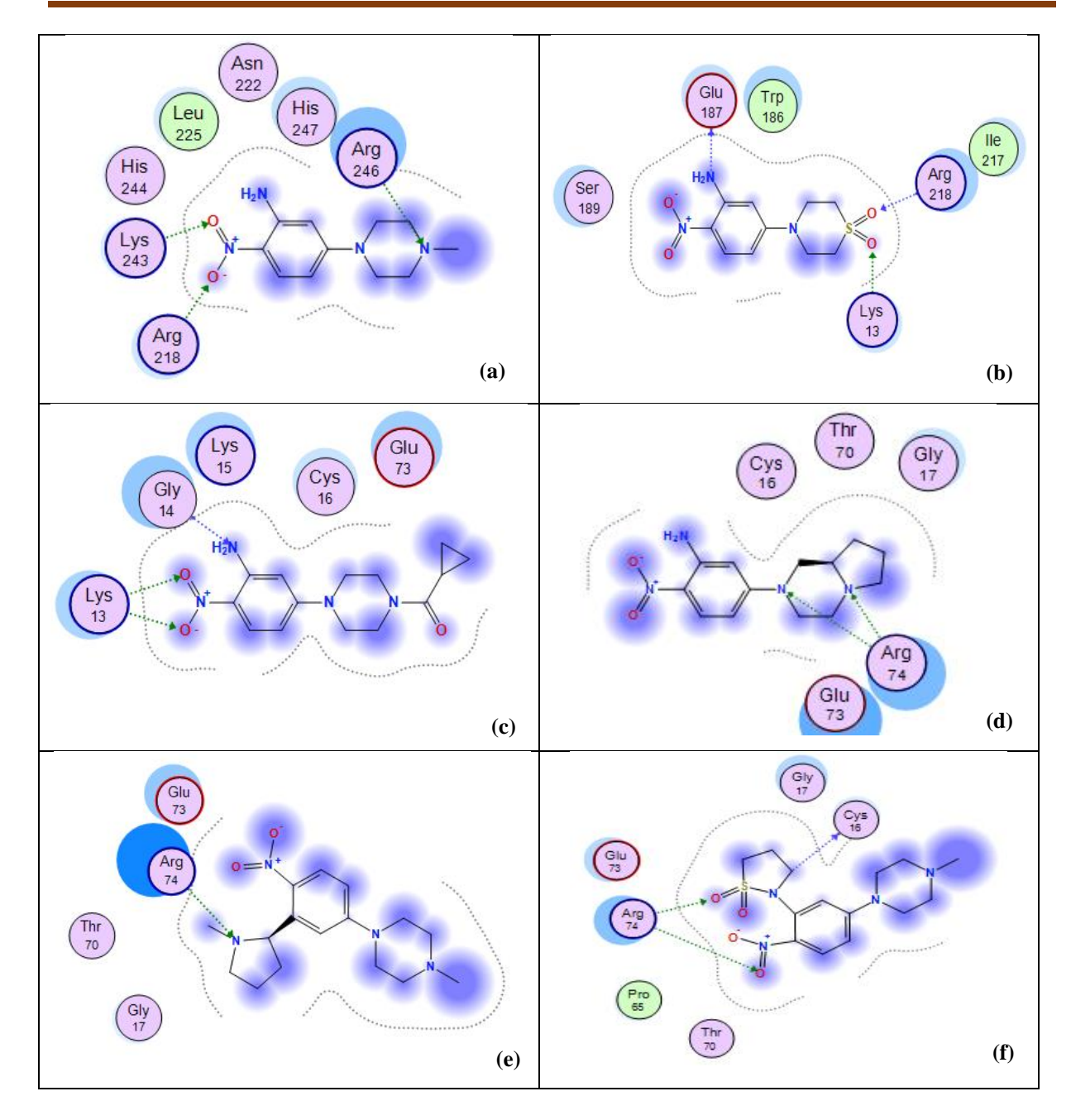


Figure III. 9 : 2D interactions formed after molecular Dynamics simulation between the synthesized compound and the best analogs (L1, L4, L13, L17 and L18) with the active site residues of the SIRT6 receptor (3K35).

It is apparent that the synthesized compound established four hydrogen bonds with the active site of the 3K35 target: H-acceptor with ARG 246, H-acceptor with LYS 243 and two strong H-acceptors with ARG 218, (distances: 3.33, 3.34, 2.98 and 2.95 Å, respectively) (Figure III.9).

Compound L1 forms H-donor bonds with GLU 187, H-acceptor with LYS 13 and H-acceptor with ARG 218 at distances between 3.03 Å and 3.35 Å, reflecting moderate interactions with active site residues. These interactions impart moderate structural stability to the 3K35-L1 complex (see Figure III.9-b).

In the 3K35-L4 complex, the ligand interacts with GLY 14 (H-acceptor, 2.88 Å) and twice H-acceptor interactions with LYS 13 at distances of 3.24 Å and 3.05 Å. These bonds demonstrate the excellent stability of the complex (see Figure III.9-c).

The compound L13 forms two H-acceptor bonds with ARG 74. The distances of these bonds, 3.29 Å and 3.15 Å, confirm the importance of ARG 74 in ligand binding and complex stability (see Figure III.9-d).

In the 3K35-L17 complex, the ligand forms acceptor hydrogen bonds with ARG 74, with distances of 2.84 (see Figure III.9-e).

Finally, the 3K35-L18 complex shows a significant H-donor interaction with ARG74 (2.67 Å) and H-acceptor interaction with GLU 73 (3.17 Å). These interactions established in this complex illustrate its good conformational stability (see Figure III.9-f).

III.3.2.4. Evaluation of the ADME properties and drug-likeness:

Currently, ADME pharmacological properties play an important role in the development of new orally administered drugs. Bioavailability parameters used to evaluate the ADME properties of drug molecules include lipophilicity, molecular weight, topological polar surface area, solubility, number of rotational bonds, and donor/acceptor hydrogen bonds. For a drug to be bioavailable, it must satisfy the various bioavailability rules, namely Lipinski's rule (- MW \leq 500 - Log P \leq 5 - HBA \leq 10 - HBD \leq 5) [32], Veber's rule (- TPSA \leq 140 - Number of rotational bonds \leq 10- HBA \leq 12 - HBD \leq 12) [33].

A study of ADME parameters was performed on the synthesized compound and five best analogs.

Table III. 5: ADME and Drug likeness properties for the synthesized compound and five best analogs.

Category	Model		Synthesized molecule	L1	L4	L13	L17	L18	Co-crystallized ligand (APR)
ies	Foi	rmula	$ m C_{11}H_{16}N_4O_2$	C ₁₀ H ₁₃ N ₃ O ₄ S	C ₁₄ H ₁₈ N ₄ O ₃	C ₁₃ H ₁₈ N ₄ O ₂	C ₁₆ H ₂₄ N ₄ O ₂	$C_{14}H_{20}N_4O_4S$	$\mathrm{C}_{15}\mathrm{H}_{23}\mathrm{N}_5\mathrm{O}_{14}\mathrm{P}_2$
Physicochemical properties		lar weight /mol)	236.27	271.29	290.32	262.31	304.39	340.40	559.32
hemical		PSA Ų)	78.32	117.60	95.39	78.32	55.54	98.06	311.14
sicoc	Num. H-bo	ond acceptors	3	4	3	3	4	5	17
Phy	Num. H-l	ond donors	1	1	1	1	0	0	8
	Num. He	Num. Heavy atoms		18	6	6	6	23	9
	Num. Rot	atable bonds	2	2	4	2	3	3	9
	Water solubility		Soluble	Soluble	Soluble	Soluble	Soluble	Soluble	Highly soluble
Lipophilicity	Log p(o/w)		0.09	-0.36	0.43	0.64	1.14	-0.04	-4.48
	ption	GI absorption	High	High	High	High	High	High	Low
	Absorption	P-gp substrate	NO	NO	YES	YES	YES	YES	YES
Pharmacokinetics	Distribution	BBB	NO	NO	NO	NO	YES	NO	NO
harm		CYP1A2	YES	YES	YES	NO	NO	NO	NO
콥	sm	CYP2C19	NO	NO	NO	NO	YES	YES	NO
	Metabolism	CYP2C9	NO	NO	NO	NO	NO	NO	NO
	Met	CYP2D6	NO	NO	NO	NO	YES	NO	NO
		CYP3A4	NO	NO	NO	NO	NO	NO	NO

Drug likeness	Lipinski	YES	YES	YES	YES	YES	YES	NO 3 violations MW>500, NorO>10, NHorOH>5
	Veber	YES	YES	YES	YES	YES	YES	NO 1 violation: TPSA>140

The results in Table III.5 show that the synthesized molecule and its analogs: L1, L4, L13, L17 and L18, have satisfactory pharmacokinetic profiles, making them suitable for consideration as potential drug candidates against the SIRT6 (3K35) target.

First, all compounds show high gastrointestinal (GI) absorption, an essential criterion for good oral bioavailability. Molecular weights are all below 500 g/mol, which favors penetration across cell membranes and thus a good absorption profile. It also appears that compounds L4, L13, L17 and L18 were found to be P-gp substrates, except the synthesized compound and L1.

The most significant feature of these compounds is their TPSA values (below 140 Å²), which are also applicable in this case and are often used as a criterion to evaluate a molecule's ability to penetrate the blood-brain barrier. The number of hydrogen bond donors (\leq 2) and acceptors (\leq 8) are in accordance with Lipinski's rules, supporting their orally active potential. Log P values are moderate (from -0.36 for L1 to 1.14 for L17), ensuring a balance between aqueous solubility and lipid permeability, favorable for efficient tissue distribution.

Additionally, the compounds under study have a desirable drug-likeness profile, as seen by their perfect adherence to the Lipinski and Veber criteria (Table III.5).

Furthermore, all compounds are predicted to be unable to cross the blood-brain barrier (BBB). However, these compounds are unable to penetrate the central nervous system (CNS), except for the compound L17, which has BBB permeability.

According to the CYP450 isoform prediction, all substances are predicted to act as non-inhibitors of CYP2C9 and CYP3A4.

On the other hand, the co-crystallized ligand (APR) does not satisfy the drug-likeness and ADME parameters. Given its high-water solubility and high hydrophilicity (logP = -4.48), this molecule has been unable to penetrate through lipid barriers and reach its biological target (Table III.5).

References

- [1] Meng, X.-Y., Zhang, H.-X., Mezei, M., & Cui, M. Molecular docking: A powerfulapproach for structure-based drug discovery. Current Computer-Aided Drug Design.2011, 7(2), 146–157.
- [2] WeiningSuna,c, XiuliChenb,c, Shenzhen Huangb, Wenpei Lib, Chenyu Tiana, ShengyongYangb,LinliLia,Discovery of 5-(4-methylpiperazin-1-yl)-2-nitroaniline derivatives as a new class of SIRT6 inhibitors.
- [4] Fan J, Fu A, Zhang L. Quant Biol. 2019;7:83. doi: 10.1007/s40484-019-0172-y.
- [5] Pagadala NS, Syed K, Tuszynski J. BiophysRev. 2017; 9:91. doi: 10.1007/s12551-016-0247-1
- [6] Tripathi A, Bankaitis VA. J Mol Med Clin Appl. 2017;2:19. doi: 10.16966/2575-0305.106.
- [7] O'Boyle, N. M., Banck, M., James, C. A., Morley, C., Vandermeersch, T., & Hutchison, G. R. Open Babel: An open chemical toolbox. Journal of Cheminformatics. 2011, 3, 33.
- [8] Dolinsky, T. J., Nielsen, J. E., McCammon, J. A., & Baker, N. A. PDB2PQR: An automated pipeline for the setup of Poisson–Boltzmann electrostatics calculations. Nucleic Acids Research, 32(Web Server issue), W665–W667,2004.
- [9] Volkamer, A., Kuhn, D., Grombacher, T., Rippmann, F., &Rarey, M. Combining global and local measures for structure-based druggability predictions. Journal of Chemical Information and Modeling.2012, 52(2), 360–372.
- [10] Genheden, S., & Ryde, U. The MM/PBSA and MM/GBSA methods to estimate ligand-binding affinities. Expert Opinion on Drug Discovery.2015,10(5), 449–461.
- [11] Xu, D., & Zhang, Y. Improving the physical realism and structural accuracy of protein models by a two-step atomic-level energy minimization. Biophysical Journal, 2011, 101(10), 2525–2534
- [12] Nicholls, A., Sharp, K. A., & Honig, B. Protein folding and association: Insights from the interfacial and thermoDynamics properties of hydrocarbons. Proteins: Structure, Function, and Genetics.1991,11(4), 281–296.
- [13] Frenkel, D., Smit, B., & Ratner, M. A. Understanding molecular simulation: from algorithms to applications (Vol. 2). San Diego: Academic press.1996.
- [14] Jarosaw, M. Molecular Dynamics, Cornell University, Ithaca, New York, USA Nicholas Copernicus University Torun, Poland
- [15] Henry Jakubowski A. Benedict/St. John's. Introduction to Molecular Mechanics and Molecular Dynamics Text. University.2021.
- [16] M Wagener and JP Lommerse. The quest for bioisosteric replacements. Journal of Chemical Information and Modeling.2006, 46:677–685
- [17] J. Shan and C Ji. Molopt: a web server for drug design using bioisosteric transformation. Current Computer-Aided Drug Design.2020,16:460–466
- [18] Yagoub Oum Hani, R. A. I. Modélisation moléculaire pour la découverte de nouveaux inhibiteurs de caspase-3.2021.

- [19] Shuang Zhao, Yan-Yan Zhu, Xiao-YuWang, Yong-Sheng Liu, Yun-Xiang Sun, Qing-Jie Zhao, and Hui-Yu Li, Article Structural Insight into the Interactions between Structurally Similar Inhibitors and SIRT6
- [20] Christine Schlicker, Gina Boanca, Mahadevan Lakshminarasimhan, and Clemens Steegborn, Structure-based development of novel sirtuin inhibitors
- [21] Chemical Computing Group Inc. Molecular operating environment (moe),
- [22] Bond SD, Leimkuhler BJ, Laird BB. The Nosé–Poincaré Method for Constant Temperature Molecular Dynamics. Journal of Computational Physics.1999, 151:114–134. https://doi.org/10.1006/jcph.1998.6171
- [23] Sturgeon JB, Laird BB. Symplectic algorithm for constant-pressure molecular Dynamics using a Nosé–Poincaré thermostat. The Journal of Chemical Physics.2000, 112:3474–3482. https://doi.org/10.1063/1.480502
- [24] Parikesit AA, zahroh H, Nugroho AS, et al. The Computation of Cyclic Peptide with Prolin-Prolin Bond as Fusion Inhibitor of DENV Envelope Protein through Molecular Docking and Molecular Dynamics Simulation. arXiv:151101388 [q-bio]. https://doi.org/10.13140/2.1.4133.3760
- [25] Berendsen HJC, Postma JPM, van Gunsteren WF, et al (1984) Molecular Dynamics with coupling to an external bath. The Journal of Chemical Physics.2015, 81:3684–3690. https://doi.org/10.1063/1.448118
- [26] Origin (Pro), OriginLab Corporation, Northampton, MA, USA. Version 2021.
- [27] A. Daina, O. Michielin, and V. Zoete. Swissadme: a free web tool to evaluate pharmacokinetics, drug-likeness and medicinal chemistry friendliness of small molecules. Scientific Reports, 2017, 7:1–13
- [28] A. Imberty, KD Hardman, JP Carver, and S Perez. Molecular modeling of protein-carbohydrate interactions. docking of monosaccharides in the binding site of concanavalin a. Glycobiology.1991, 1(6):631–642
- [29] C Janiak. A critical account on n-n stacking in metal complexes with aromatic nitrogen-containing ligands. Journal of the Chemical Society, Dalton Transactions, 2000, (21):3885–3896.
- [30] SK Burley and GA Petsko. Aromatic-aromatic interaction: a mechanism of protein structure stabilization. Science, 1985, 229(4708):23–28.
- [31] D. Piovesan, G. Minervini, and SCE Tosatto. The ring 2.0 web server for high quality residue interaction networks. Nucleic Acids Research, 44(W1): W367–W374, 2016.
- [32] Lipinski, Christopher A., et al. "Experimental and computational approaches to estimate solubility and permeability in drug discovery and development settings." Advanced drug delivery reviews.19997, 23.1-3.3-25.
- [33] Veber, Daniel F., et al. "Molecular properties that influence the oral bioavailability of drug candidates." Journal of medicinalchemistry.2002, 45.12 2615-2623.

GENERAL CONCLUSION

This Master's thesis takes an integrated approach, combining theoretical chemistry (DFT) and molecular modeling for drug discovery. This approach aims to better understand the electronic reactivity and pharmacological potential of 2-nitroaniline derivatives.

The first part of this study investigated the regioselectivity of the transetherification reaction on 4,5-Dialkoxy-2-nitroanilines using the DFT method based on the experimental results obtained by Jarosław Grolik et al. (2022). Theoretical approaches, such as frontier molecular orbitals (FMO), molecular electrostatic potential (MEP), Fukui indices, and global and local reactivity indices, were employed to study the electronic distribution of the molecule. The analysis revealed that the para (C4) position is the preferred site for nucleophilic attack due to electronic accessibility. This study rationalizes the reaction selectivity of this molecule and provides a basis for designing functional derivatives useful in organic synthesis and pharmacochemistry.

The second part of the study focused on investigating the inhibitory properties of 5-(4-methylpiperazin-1-yl)-2-nitrobenzylamine on the SIRT6 protein using molecular modeling approaches. This molecule has been synthesized and evaluated for its high antidiabetic activity. This molecule and its structural analogs (L1, L4, L13, L17, and L18) interact with the SIRT6 receptor pocket (PDB: 3K35), which is known for its role in regulating metabolism, aging, and diabetes. The molecular docking study identified that L4 and L18 as the compounds with the best binding energy scores (-8.17 and -7.43 kcal/mol), as well as strong interactions with the active residues of the active pockets of 3K35.

Molecular Dynamics simulations confirmed the structural stability of the formed complexes, particularly for L4 and L18, with stabilized potential energies over 1000 ps of simulation. ADME and drug-likeness studies showed that these compounds met the Lipinski and Veber criteria. They have good gastrointestinal absorption, adequate solubility, and a favourable metabolic profile, making them suitable for oral administration.

The results suggest that compounds L4 and L18 warrant further development as potential SIRT6 inhibitors and offer promising prospects for the rational design of targeted drugs.